
**Index**

| | | |
|---|---|---|
| **13** | Contrasting effects of anodal and cathodal high-definition TDCS on proprioceptive responses in sensorimotor cortex, measured with MEG during voluntary finger | Jed A. Meltzer |
| **14** | Modulation of TMS-evoked transcallosal inhibition by voluntary hand movement | Sabira Alibhai-Najarali |
| **15** | Music-based fine motor rehabilitation in Parkinson's patients: feasibility, efficacy and neural correlates | Isabelle Buard PhD |
| **16** | Magnetoencephalographic Correlates of Reward Processing in Mood Disorders | Amy Xu |
| **17** | Phenotype of frontal lobe glioma determines the frequency band specific functional connectivity alteration | Apisit Kaewsanit |
| **18** | ASD and TD individuals show increased cortical responses to shift in sound source during a spatial hearing task | Sergio Osorio |
| **19** | The Balance Between Top-Down and Bottom-Up Attention in Misophonia | Jasmine Tan |
| **20** | Novel clinical MEG/MSI approach to detect and localize the subtle and non-localizing epileptogenic events. | Velmurugan Jayabal |
| **21** | Advanced MEG Data Processing in Epilepsy Patients with RNS | Pegah Askari |
| **22** | Altered gamma power oscillations in patients with comorbid temporal lobe epilepsy and psychiatric disorders: a novel MEG spectral analysis | Natascha Cardoso da Fonseca |
| **23** | MEG and Repetitive Head Impact Exposure in Youth Football Players | Natalie M. Bell |
| **24** | Temporal signatures of multidimensional object properties in the human brain | Lina Teichmann |
| **25** | Decoding Individual sequence skill learning actions during planning and execution | Debadatta Dash |
| **26** | Temporal Dynamics of Age, Gender, and Identity Representations Invariant to Head Views for Familiar Faces | Amita Giri |
| **27** | Temporal Characteristics of Mental Imagery | Sebastian Montesinos |
| **28** | Load-dependent and capacity-limited response in the posterior parietal cortex during visual working memory retention: MEG evidence | Xinchi Yu |
| **29** | Exploring Working Memory Networks using Hidden Markov Models | Shivam Bansal |
| **30** | Estimating the Number of Active Sources in MEG Based on an F-ratio Method | Amita Giri |
| **31** | Multi-Modal Deep Fusion Neural Networks for Brain Source Imaging Based on EEG and MEG | Meng Jiao |
| **32** | Bayesian Inference for Brain Source Imaging with Structured Low-rank Noise | Sanjay Ghosh |
| **33** | Reliable MEG/MSI source localization in patients with implanted vagus nerve stimulator (VNS) devices: a single-centered, large clinical observation study | Mahmoud Jiha |
| **34** | Validation of a novel hand-squeezing paradigm for quantification of interhemispheric inhibition (IHI) between motor cortices using MEG | Alica Rogojin |
| **35** | Multi-Frequency Encoded Source Imaging for Wearable OPM-MEG | J Xiang |
| **36** | Biplanar coil cancellation system for OPM-MEG using PCB | Mainak Jas |
| **37** | OPM-MEG vs. SQUID-MEG in Epileptic Source Localization: A Cost-Effective Alternative | Tyrell Pruitt |
| **38** | Towards precise mapping of digit representations in the human somatosensory cortex with high resolution magnetoencephalography | Amaia Benitez Andonegui |

# Neural Tracking Measures of Speech Intelligibility: Manipulating Intelligibility while Keeping Acoustics Unchanged

I.M Dushyanthi Karunathilake[1], Joshua P. Kulasingham[2], Jonathan Z. Simon[1,3,4]

[1]*Department of Electrical and Computer Engineering, University of Maryland, College Park, MD 20742, USA*
[2]*Department of Electrical Engineering, Linköping University, Linköping, SE*
[3]*Institute for Systems Research, University of Maryland, College Park, MD 20742, USA*
[4]*Department of Biology, University of Maryland, College Park, MD 20742, USA*

Neural speech tracking has advanced our understanding of how our brains rapidly map an acoustic speech signal onto linguistic representations and ultimately meaning. However, it remains unclear which aspects of the corresponding neural responses correspond to speech intelligibility, which is only loosely coupled to the acoustics. Intelligibility related neuro-markers derived from such neural responses would play a crucial role in advancing our understanding of the neurophysiology of the speech understanding, evaluation of auditory function across diverse clinical populations, and hearing device evaluation. Many studies addressing this question vary the level of intelligibility by manipulating the acoustic waveform, making it difficult to cleanly distinguish effects of intelligibility from the underlying acoustical confounds. In this study, speech intelligibility is manipulated while keeping the acoustical structure unchanged, using degraded speech plus a priming paradigm. Acoustically identical three-band noise vocoded (degraded) speech segments (~20 s duration) are presented twice, but the second presentation is preceded by the original (non-degraded) version of the same speech segment. This priming, which generates a 'pop-out' percept, substantially improves the intelligibility of the second presentation of the degraded speech passage while keeping the acoustics identical. We recorded magnetoencephalography (MEG) data from 25 younger adults and investigated how intelligibility affects auditory and linguistic neural tracking measures using multivariate Temporal Response Functions (mTRFs). As expected, behavioral results confirmed that perceived speech clarity is improved by priming. mTRF analysis revealed that auditory (speech envelope and envelope onset) and phoneme onset neural responses are influenced only by the acoustics of the sensory input (bottom-up driven mechanisms). Critically, our key findings suggest that neural measures associated with the segmentation of sounds into words emerges first with better speech intelligibility, especially those time-locked at N400-like latencies in prefrontal cortex (PFC), in line with engagement of top-down mechanisms associated with priming. Taken together, our results suggest that time locked neural responses associated with lexical segmentation may serve as novel objective measures of speech intelligibility.

This work was supported by the National Institutes of Health grant R01-DC019394 and National Science Foundation grant SMA 1734892

# Tinnitus percept is associated with magnetoencephalography-derived measures of resting state connectivity between temporal and frontal cortices

Corby L Dale[1], Leighton BN Hinkley[1], Jennifer Henderson-Sabes[2,3], Cole Davis[4], Abhishek Bhutada[1,5], Lingwei Ouyang[1,6], Andrew P Walther[1,7], Wenbo Zhang[4], Meredith E Adams[8], Srikantan S Nagarajan[1,2,9], Steven W Cheung[2,10]

[1] Department of Radiology and Biomedical Imaging, University of California San Francisco
[2] Department of Otolaryngology—Head and Neck Surgery, University of California San Francisco
[3] University of the Pacific, Department of Audiology
[4] Minnesota Epilepsy Group, John Nasseff Neuroscience Center at United Hospital in St. Paul, MN
[5] Graduate School of Medicine, Virginia Tech
[6] Graduate program in Psychology, University of Texas at Austin.
[7] Summer undergraduate intern program, ci2 Center for Intelligent Imaging, University of California San Francisco
[8] Department of Otolaryngology—Head and Neck Surgery, University of Minnesota
[9] UCB-UCSF joint program in Bioengineering and Therapeutic Sciences
[10] Surgical Services, Department of Veterans Affairs, San Francisco.

Subjective tinnitus refers to conscious perception of sound for which no external auditory stimulus is identified. Models of tinnitus postulate increased connectivity between auditory cortex and basal ganglia, limbic areas, or frontal areas. Brain imaging may objectively determine presence and magnitude of percept and assist in understanding underlying physiology.

At one of 2 study sites, 380 adults with (N = 185) and without (N = 195) tinnitus underwent 5 minutes of task-free eyes-closed magnetoencephalography (MEG), structural imaging (MRI), audiometry, and tinnitus assessment (TFI). A subset (N=44) repeated the study. Source imaging localized 1 to 4 minutes of MEG activity within brain anatomy. Voxel-based activity, parsed into 6 frequency bands and spatially-normalized, was mapped to 246 Brainnetome atlas regions. Imaginary coherence (ImCoh) and directional phase transfer entropy (dnPTE) were calculated between each unique pair of regions. Analysis of variance (rmANOVA), repeated across frequency with group, age, and site, provided F-ratios and FDR-corrected p-values for pairwise connectivity, as well as relation to TFI. Binomial linear regression queried contribution of band to group effects. Linear discriminant analysis with 10-fold cross validation assessed potential for classification.

Groups differed at 4 pairs out of 30,012 queried. Using ImCoh, tinnitus exhibited increased slow oscillatory connectivity between regions in left temporal and right frontal cortex (LPHG-RIFC: $F=9.00$, $p<.01$) and (LITC-ROFC: $F=9.04$, $p<.01$), driven by delta (1 - 3 Hz, LPHG-RIFG: $B = 25.8$, $t=4.21$; LITC-ROFC: $B = 15.6$, $t=3.14$, both $p<.01$). For dnPTE, tinnitus showed decreases in intrahemispheric high gamma (63 – 117 Hz) connectivity between portions of cingulate and parietal cortex (Left: $F=12.4$, $B = -1.16$, $t=-4.67$, $p<.01$; Right: $F=12.31$, $B = -1.16$, $t=-3.97$, $p<.01$). Using connectivity of these pairs in identified bands as classifiers produced acceptable levels of diagnostic performance (AUC =.74 [.68 - .78]). TFI scores changed from Session 1 to 2 (paired $t=2.13$, $p=.045$), but with considerable distribution overlap (K-S test, $K=.27$, $p=.33$).

Tinnitus-related differences in connectivity can adequately classify tinnitus and non-tinnitus participants. Commonalities among these 4 regions may further our understanding of the underlying physiology of tinnitus. Paradoxically, group connectivity differences did not relate to subjective scores used to diagnose tinnitus. However, TFI appeared to change from session-to-session, while connectivity largely did not, indicating that neural measures of tinnitus may be more stable than subjective measures.

# Left fusiform activity explains variability in fixation durations during natural reading: Evidence from co-registered MEG & eye-tracking

Graham Flick[1,2] & Liina Pylkkänen[1]

1. New York University, USA 2. Rotman Research Institute, Baycrest Centre, Canada

**Introduction:** Eye movements during reading are influenced by the linguistic and cognitive demands of what is being read, indicating that brain networks controlling eye movements, and those controlling the recognition of words, must cooperate. Historically, however, neuroscientific studies of reading have tended to use rapid serial visual presentation (RSVP), thereby eliminating eye movements. This has resulted in a paucity of evidence concerning how brain activity gives rise to eye movement behavior during reading and makes it unclear if neurocognitive accounts of reading, informed by RSVP studies, generalize to the behavior of interest. Here, we used co-registered MEG and eye-tracking to examine the brain systems that support visual word recognition while participants freely read short stories with eye movements.

**Methods:** Thirty-two participants naturally read 216 short stories, each consisting of two sentences, while concurrent MEG and eye-tracking data were collected. Stories were annotated with the properties of each word (e.g., letter bigram frequency, lexical frequency, surprisal), enabling us to identify brain responses, time-locked to fixations, that were modulated by these properties. Responses were analyzed using linear deconvolution to disentangle overlapping activity and localized to the cortical surface using minimum norm estimation with high resolution anatomical MRIs. Linear mixed effects models and nested model comparisons were used to identify neural responses that correlated with each property of the fixated words and to identify brain responses that explained variability in the duration of fixations before they terminated, beyond what could be explained by psycholinguistic properties of the words alone. Finally, in a follow-up study, a separate sample of participants read the same short stories presented one-word-at-a-time in RSVP, allowing us to compare the influence of word properties on brain responses across the two reading modalities.

**Results:** We first replicated past results demonstrating that a progression of left occipitotemporal activity supports visual word recognition. We then examined where in this progression each of the properties of fixated words modulated responses. During natural reading, word length correlated with activity in primary visual cortex bilaterally (50-200 ms) while lexical frequency correlated with activity in the left fusiform gyrus (100-170 ms after fixation onset). In contrast, letter bigram frequency and lexical surprisal did not correlate with responses in the ventral visual word pathway. We next extracted responses from occipitotemporal areas and asked if activity at these stages correlated with how long the eyes lingered on the currently fixated word – possibly indicating that word processing at this stage influences oculomotor control. Consistent with the proposal that it houses a bottleneck on visual word recognition, the left fusiform gyrus showed this pattern, with longer fixations associated with more negative amplitudes, shortly after fixation onset. Finally, a comparison of natural reading versus RSVP revealed a stark contrast in how word frequency and surprisal correlated with brain activity across the two paradigms, with widespread correlations between these properties and brain activity observed only in the slower, one-word-at-a-time RSVP reading.

**Changes in Cortical Directional Connectivity during Difficult Listening in Younger and Older Adults**

Behrad Soleimani[1,2], I.M. Dushyanthi Karunathilake[1,2], Proloy Das[3], Stefanie E. Kuchinsky[4], Behtash Babadi[1,2], Jonathan Z. Simon[1,2,5]

[1]Department of Electrical and Computer Engineering, University of Maryland, College Park, MD 20742, USA
[2]Institute for Systems Research, University of Maryland, College Park, MD, 20742, USA
[3]Department of Anesthesia, Critical Care and Pain Medicine, Massachusetts General Hospital, Boston, MA, 02114, USA
[4]Audiology and Speech Pathology Center, Walter Reed National Military Medical Center, Bethesda, MD, 20889, USA
[5]Department of Biology, University of Maryland College Park, MD, 20742, USA

Fully understanding the neural underpinnings of speech comprehension in difficult listening conditions requires understanding the concurrent cortical connectivity. Granger causality is a useful measure of connectivity, typically employed in functional magnetic resonance imaging (fMRI) studies, but the limited temporal resolution of fMRI restricts the capture of higher frequency neural interactions crucial for complex speech processing. On the other hand, although magnetoencephalography (MEG) can capture neural interactions at the millisecond scale, its limited spatial resolution poses challenges in conventional connectivity analyses. A recently proposed cortical connectivity analysis methodology, network localized Granger causality (NLGC), can extract Granger causal interactions in MEG data without the need for any intermediate source-localization step. This one-shot approach also effectively addresses challenges related to false alarms and localization errors, providing a robust assessment of cortical connectivity. In this study, NLGC is applied to MEG recordings from younger and older adults while performing a speech listening task with varying background noise conditions. The analysis focuses on directional cortical connectivity patterns within and between the frontal, temporal, and parietal lobes, specifically in the delta and theta frequency bands. The results demonstrate significant age- and condition-related connectivity differences, particularly in the theta band. In younger adults, increasing background noise leads to a shift from predominantly temporal-to-frontal (bottom-up) connections for clean speech to dominantly frontal-to-temporal (top-down) connections in noisy conditions. In contrast, older adults exhibit bidirectional information flow between frontal and temporal cortices regardless of the background noise. Furthermore, NLGC allows classification of connections as either excitatory or inhibitory based on their temporal relationships, enabling a more nuanced understanding of the neural mechanisms involved in speech perception. While delta band connection types show no significant age-related changes, theta band connection types exhibit substantial changes in excitation/inhibition balance across age and condition. Supported by the National Institutes of Health (P01-AG055365, R01-DC019394) and the National Science Foundation (SMA 1734892, OISE 2020624, CCF 1552946).

# Cortical Responses Time-Locked to Continuous Speech in the High-Gamma Band Depend on Selective Attention

V. COMMURI[1], J. KULASINGHAM[2], J. Z. SIMON[1];

[1]Electrical and Computer Engineering, University of Maryland, Col. Park, College Park, MD;
[2]Department of Electrical Engineering, Linköping University, Linköping, SE

Auditory cortical responses to speech obtained by magnetoencephalography (MEG) show robust speech tracking in the high-gamma band (70-200 Hz), but little is currently known about whether such responses depend at all on the focus of selective attention. In this study we investigate differences in high-gamma cortical responses to male and female speech, and we address whether these responses, thought to originate from primary auditory cortex, depend on selective attention. Twenty-two human subjects listened to concurrent speech from male and female speakers and selectively attended to one speaker at a time while their neural responses were recorded with MEG. The male speaker's pitch range coincided with the lower range of the high-gamma band. In contrast, the female speaker's pitch range was higher, and only overlapped the upper end of the high-gamma band. Neural responses were analyzed using the temporal response function (TRF) framework. As expected, the responses demonstrate robust speech tracking in the high gamma band, but only to the male's speech. Responses present with a peak latency of approximately 40 ms indicating an origin of primary auditory cortex. The response magnitude also depends on selective attention: the response to the male speaker is significantly greater when male speech is attended than when it is not attended. This is a clear demonstration that even very early cortical auditory responses are influenced by top-down, cognitive, neural processing mechanisms. Supported by the National Institutes of Health (R01-DC019394) and the (National Science Foundation (SMA 1734892).

# Localizing covert and overt picture naming processes using MEG

**Wei H.T.**[1,2*], Faisal F.B.[1], Shao C.[1], Beck T.[1], Meltzer J.A.[1,2]
[1]Rotman Research, Baycrest Hospital; [2]Psychology, University of Toronto

## Background

Numerous hemodynamic studies have mapped out brain regions involved in the process of naming. Nonetheless, the higher temporal resolution in an electrophysiological signal is crucial for identifying the latency and relative order of different word retrieval stages (e.g., lemma selection, phonological activation, etc.). Although several studies have reported event-related potentials time-locked to naming events, fewer studies have investigated modulation of neuronal oscillations both phase-locked and non-phase-locked to picture naming processes. Furthermore, methodological differences in naming paradigm and data processing for the removal of motor artefacts remain critical issues across language production studies. These difficulties identified in the literature call for comparisons between naming methods, as well as the need for valid paradigms eliciting word retrieval processes while avoiding motor artefacts.

## Objectives

This MEG study (1) examines the **loci and power modulations underlying semantic interference and phonological facilitation** during covert picture naming, and (2) highlights the similarities and differences in **oscillatory modulations across different covert and overt naming** tasks.

## Method

Thirty young healthy adults (22.73 ± 4.36; 20 female) participated in a structural MRI and three picture naming tasks under MEG. Aside from the traditional **overt picture naming**, we included two covert picture naming tasks. One was a **covert picture-word interference (PWI) task** where participants were instructed to ignore the audio distractor word and focus on judging whether the target picture name ends in a target sound assigned for the block by pressing yes/no buttons. By manipulating the semantic and phonological relations between distractor words and target pictures, the covert PWI task was previously validated to elicit both semantic interference (SI) and phonological facilitation (PF) at distinct stages of word retrieval, suggested by distinct optimal onset asynchronies (Wei et al, 2022). The covert PWI also included a "no distractor condition" that was simply **an ending sound matching** task. The other covert naming task required participants to judge whether the target picture name begins with the target sound assigned for the block by pressing yes/no buttons. The **beginning sound matching** design was intended for potential application with stroke patients, as it is an easier task.

## Results

Participants performed comparably in overt naming and beginning sound matching tasks, with both being faster and more accurate than the PWI task, in which the SI slowing and PF speeding effects were observed. (Objective 1:) In the MEG source-level data, **semantic interference** during naming was associated with **alpha power decrease** in the frontal, temporal, and inferior parietal regions in both hemispheres, suggesting extra cortical engagement recruited with the presence of a cued competitor for target naming. On the other hand, **phonological facilitation** in naming was accompanied by **alpha power increase** across bilateral frontal and perisylvian regions, reflecting the relative ease in name retrieval with phonological cues. (Objective 2:) Across the **covert and overt naming** tasks, the neuronal oscillations mainly **differed in the motor and occipital cortices** according to the task-specific response planning (e.g., mouth vs. hand movement; attention to beginning sound vs. full phonology activation), while retaining similar word-retrieval neuronal activities.

## Conclusion

This study characterized the **neuronal oscillatory modulations underlying interference and facilitation effects during covert naming**. Furthermore, by demonstrating that the main neurophysiological deviation of covert from overt naming lies in the response preparation and visual recognition aspects, the results suggested **promising validity of using the covert naming designs to probe word retrieval processes without verbal motor artefacts** in laboratory settings.

**An Experimental Methods Based Approach to Understanding the Mechanisms Underlying MEG Indices of Auditory/Language Processing**

Miguel Jaime[1], Lindsay M Oberman[1], Sunday M Francis[1], Jeff Stout[1], Zhi-De Deng[1], Pei Robins[1], Jan Willem van der Veen[1], Sarah H Lisanby[1]

[1]National Institute of Mental Health

**Background:**
Language/auditory processing deficits are a hallmark feature of autism spectrum disorder (ASD). Magnetoencephalography (MEG) studies have shown delayed M100 auditory evoked field responses and altered induced gamma-band activity in individuals with ASD. MEG indices of language/auditory processing, as a result, have been proposed as putative biomarkers for ASD. The mechanisms underlying these aberrant MEG measures, however, are not clearly understood. Excitatory/Inhibitory (E/I) imbalance has been suggested as a potential explanation for these deficits and the general pathophysiology of ASD. Abnormal structural and functional network connectivity have similarly been associated with language deficits in children with ASD. The current study utilizes an experimental therapeutics approach to better understand how mechanisms of E/I balance and structural and functional network connectivity contribute to MEG outcomes of language/auditory processing in ASD. Here, we present data from the healthy volunteer pilot phase of this study, investigating how measures of E/I balance, structural connectivity, and functional connectivity are related to MEG measures of language/auditory processing.

**Methods:**
Twenty healthy adult volunteers completed MEG, MRI, functional MRI (fMRI), and Magnetic Resonance Spectroscopy (MRS) at baseline and then immediately before and after continuous theta burst stimulation (cTBS) applied at 80% active motor threshold. Brain stimulation targets were individualized and determined by peak BOLD activation during an fMRI language-based task. fMRI data were additionally processed to measure task-based functional connectivity between the left posterior superior temporal cortex (psTC) and left frontal language areas. Diffusion weighted imaging (DWI) data were acquired and analyzed to quantify fractional anisotropy (FA), radial diffusivity (RD), mean diffusivity (MD), and axial diffusivity (AD) in specific left white matter tracts (e.g., arcuate fasciculus and auditory radiation fiber bundles). A spectroscopy voxel of 2.5 $cm^3$ was placed within the left pSTC for MRS. MRS data were then processed to measure creatine-normalized concentrations of glutamate and gamma-amino butyric acid (GABA), as well as the ratio of glutamate/GABA. MEG data were collected while participants listened to validated auditory stimuli and then processed to measure M100 latency and induced gamma power in the left pSTC.

**Results:**
M100 latency negatively correlated with glutamate [$r(n=9) = -0.907$, $p < 0.001$] and the ratio of glutamate/GABA [$r(n=9) = -0.681$, $p < 0.05$] at baseline, while changes in M100 latency positively correlated with changes in glutamate/GABA pre-post cTBS [$r(n=9) = 0.757$, $p < 0.05$]. Significant correlations ($p < 0.05$) were also observed between M100 latency and FA [$r(n=9) = 0.757$], RD [$r(n=9) = -0.767$], and MD [$r(n=9) = -0.742$] measures in the arcuate fasciculus, but none were observed between M100 latency and fMRI task-based functional connectivity. Induced gamma power negatively correlated with task-based functional connectivity [$r(n=11) = -0.678$, $p < 0.05$] at baseline but did not correlate with other MRS or DWI measures.

**Conclusions**:
These findings suggest a relationship between E/I balance, structural and functional network connectivity, and language/auditory processing in a non-clinical sample. This dataset will serve as a normative reference for our ongoing clinical study, in which we will utilize the same experimental therapeutics approach to probe these outcomes to explore how E/I balance, structural cortical architecture, and network functioning contribute to language/auditory processing in adolescents with ASD. We have begun this phase of the study and are currently enrolling.

## Laminar specificity of the auditory perceptual awareness negativity: A biophysical modeling study

*Carolina Fernandez Pujol[1*], Elizabeth G. Blundon[1,2], Andrew R. Dykstra[1]*
[1]Department of Biomedical Engineering, University of Miami, Coral Gables, FL, United States
[2]Present address: Department of Medicine, Dalhousie University, Halifax, Nova Scotia, Canada

How perception of sensory stimuli emerges from brain activity is a fundamental question of neuroscience. To date, two disparate lines of research have examined this question. On one hand, human neuroimaging studies have helped us understand the large-scale brain dynamics of perception. On the other hand, work in animal models (mice, typically) has led to fundamental insight into the micro-scale neural circuits underlying perception. However, translating such fundamental insight from animal models to humans has been challenging. Here, using biophysical modeling, we show that the auditory awareness negativity (AAN), an evoked response associated with perception of target sounds in noise, can be accounted for by synaptic input to the supragranular layers of auditory cortex (AC) that is present when target sounds are heard but absent when they are missed. This additional input likely arises from cortico-cortical feedback and/or non-lemniscal thalamic projections and targets the apical dendrites of layer-5 (L5) pyramidal neurons. In turn, this leads to increased local field potential activity, increased spiking activity in L5 pyramidal neurons, and the AAN. The results are consistent with current cellular models of conscious processing [1–3] that highlight the importance of active mechanisms in the apical dendrites of L5 pyramidal neurons [4,5] and help bridge the gap between the macro and micro levels of perception-related brain activity.

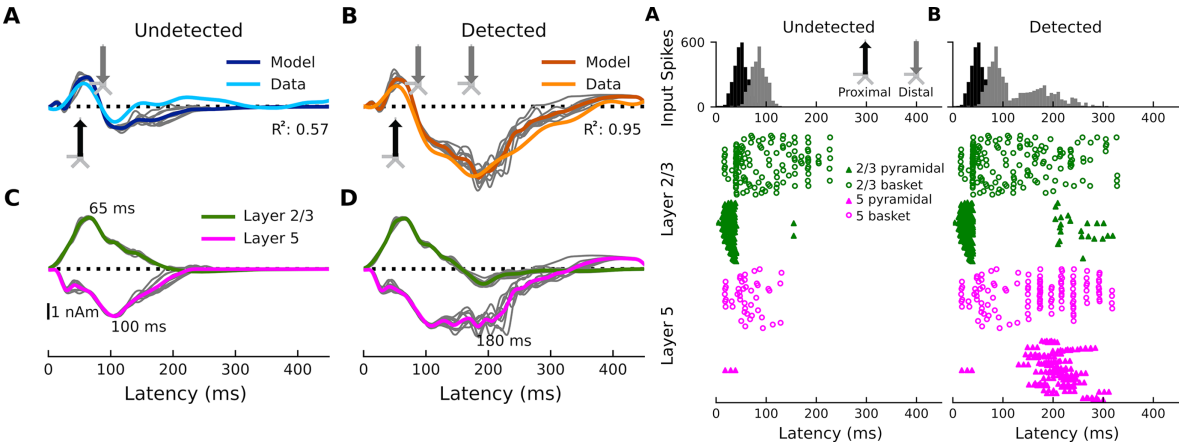


### References

1. Bachmann T, Suzuki M, Aru J. Dendritic integration theory: A thalamo-cortical theory of state and content of consciousness. 1. 2020;1.
2. Aru J, Suzuki M, Larkum ME. Cellular Mechanisms of Conscious Processing. Trends in Cognitive Sciences. 2020;24: 814–825. pmid:32855048
3. Marvan T, Polák M, Bachmann T, Phillips WA. Apical amplification—a cellular mechanism of conscious perception? Neuroscience of Consciousness. 2021;2021. pmid:34650815
4. Larkum ME, Zhu JJ, Sakmann B. A new cellular mechanism for coupling inputs arriving at different cortical layers. Nature. 1999;398: 338–341. pmid:10192334
5. Larkum ME, Wu J, Duverdin SA, Gidon A. The Guide to Dendritic Spikes of the Mammalian Cortex In Vitro and In Vivo. Neuroscience. 2022;489: 15–33. pmid:35182699

**Cassia Low Manting, MIT**

**Title: Precision tagging of neural responses for tracking selective attention & learning mechanisms in the brain**

Neural auditory steady-state responses (ASSRs) have emerged as a unique tool to separate and identify simultaneous sounds back to their respective driving stimuli, making them an ideal method for studying human cognition in complex auditory environments containing mixtures of sounds, such as in a choir or a cocktail party. ASSRs refer to the neural responses elicited by presenting an auditory stimulus at a specific frequency over time, producing a sustained oscillatory neural activity precisely at the stimulus driving frequency that can be recorded with magnetoencephalography (MEG). We showed that bottom-up and top-down attention to a specific melody within a mixture of melodies modulate the ASSR at different cortical regions. To improve sensitivity, we used a support vector machine to classify ASSRs to different attention conditions at auditory attention-related areas. Interestingly, the modulation effect by top-down attention was found to be positively correlated to individual musicality scores at the left inferior parietal lobe (IPL), while the modulation by bottom-up attention was negatively correlated to musicality at the right IPL. These results suggest that musical training can be beneficial to directing top-down attention towards a target while reducing the influence of bottom-up distractions, and that these effects are mediated by areas in the parietal cortex. Planned future studies aim to adopt a multimodal neuroimaging approach by incorporating neuroanatomical and biochemical measures, using voxel-based morphometry and magnetic resonance spectroscopy respectively, alongside MEG measurements of ASSRs. These studies will focus on investigating the neural underpinnings of auditory learning under distracting conditions, examining target- and distractor-specific responses individually as well as how their interactions affect learning.

**SVM classification of attention**

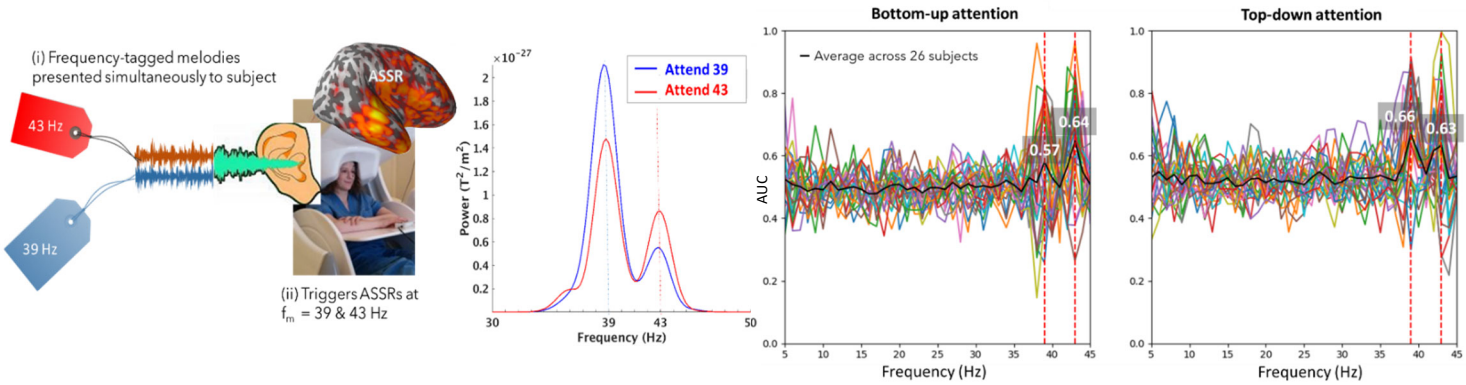


**Top-down & bottom-up attentional modulation across lobes**

| | Frontal | | Temporal | | Parietal | |
|---|---|---|---|---|---|---|
| | LH | RH | LH | RH | LH | RH |
| **Mean ASSR power modulation by a) top-down attention** | 18% | -5% | 11% | 12% | 6% | 8% |
| **$p_{one\text{-}tailed}$ (uncorrected)** | 0.0050**^ | 0.21 | 0.067 | 0.028* | 0.16 | 0.035* |

| | Frontal | | Temporal | | Parietal | |
|---|---|---|---|---|---|---|
| | LH | RH | LH | RH | LH | RH |
| **Mean ASSR power modulation by b) bottom-up attention** | 3% | 7% | 8% | 10% | 9% | 6% |
| **$p_{one\text{-}tailed}$ (uncorrected)** | 0.24 | 0.13 | 0.083 | 0.00072***^^ | 0.035* | 0.026* |

*$p < 0.001$***, $p < 0.01$**, $p < 0.05$* (uncorrected)*

*$p < 0.05$^, $p < 0.01$^^ (Bonferroni-corrected)*

**AUC vs Musicality correlation**

# Age-Related Trends in Transient Beta Bursts: Observations from Big Data

Lindsey Power, Cédric Allain, Thomas Moreau, Alexandre Gramfort, Timothy Bardouille

Human neurophysiological signals recorded by MEG consist of a series of transient bursts of neural activity with variable underlying sources and temporal characteristics. The characteristics of these bursts (e.g., burst rate, power, timing, etc.) change during task performance and throughout the normal ageing process in ways that can inform about underlying neural dynamics. In this work, we are interested in investigating the temporal and spatial characteristics of transient beta (15-30 Hz) bursts in the sensorimotor brain regions. Our objective is to identify age-related changes in these characteristics that may provide insight into functional changes in neurophysiology across the lifespan. Here, we present a novel method for source localization of transient bursts, along with a novel convolutional dictionary learning (CDL) method for transient burst detection that minimizes bias in the burst detection procedure.

We applied these methods to a large, open-access MEG dataset of over 500 healthy participants between the ages of 18-88 collected by the Cambridge Center for Ageing and Neuroscience (CamCAN). Our source localization method was used to identify the cortical sources that were most active during high-power beta bursts recorded during movement and rest. Regression analyses were then used to relate the peak source locations and regional distributions to participant age to identify age-related changes in the cortical sources of beta bursts. The analysis revealed that transient beta bursts localized to the primary sensorimotor cortices and exhibited a significant anterior shift in peak source location with age (see Figure A). These findings suggest that there is a shift in the cortical generators of beta bursts with age and that older adults may recruit additional anterior mechanisms during sensorimotor activation.

In the second part of our work, CDL was used to detect transient bursts by decomposing the signal into a convolution between a few repeating spatiotemporal patterns, called atoms, and their associated sparse activation vectors. Each atom consisted of a temporal component (i.e., a 500 ms waveform) and a spatial component (i.e., an array of weights representing the contribution of each MEG sensor to the pattern). We used CDL to extract 20 atoms for each participant and then applied an unsupervised clustering algorithm to cluster atoms across participants based on spatiotemporal similarity. This procedure allowed us to identify common signals at the group level and assess inter-subject variability and age-related trends in the characteristics of the detected atoms. The application of CDL to this dataset resulted in the detection of two distinct types of sensorimotor beta bursts with different spatial patterns (see Figure B). Age-related analyses revealed that both burst types increased in activity with age and that the increase in activity was dependent on the burst rate (i.e., number of non-zero instances of activity) rather than the burst power (i.e., magnitude of the activity). This finding provides insight to the neural mechanisms underlying age-related changes in MEG signals, suggesting that increases in beta activity with age are dependent on increases in the rate of neuronal firing rather than the size of the neuronal population.

The complimentary methods presented in this work provide a novel set of tools that can be used to probe neural transients to provide insight into functional changes in the brain. These methods together revealed the presence of multiple cortical generators of beta bursts that are dynamically related to healthy ageing.

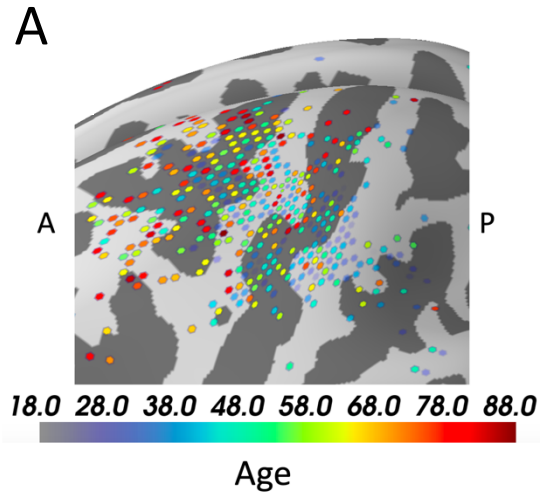


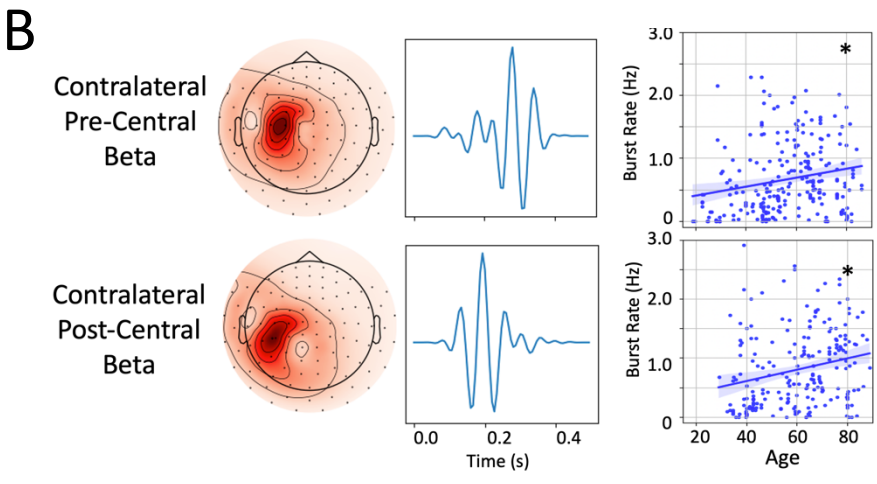

# Fully Hyperbolic Neural Networks:
# A novel approach to discover aging trajectories from MEG brain networks

Hugo Ramirez, Davide Tabarelli, Elisabeth B. Marsh, Michael Funke, John C. Mosher, Fernando Maestu, Mengjia Xu, and Dimitrios Pantazis

Characterizing age-related alterations in MEG brain networks holds great promise in understanding aging trajectories and revealing aberrant patterns of neurodegenerative disorders, such as Alzheimer's disease. Recently, graph neural network models have shown great potential in representing complex network (graph) data into embedding spaces where nodes are mapped onto low-dimensional vectors. However, the prevalent approach in graph representation learning involves embedding in the Euclidean space, which has limited representational capacity and high distortion when embedding the scale-free brain networks. In contrast, hyperbolic space, characterized by negative curvature, offers a direct solution to preserving local and global geometric information in scale-free brain graphs. This is because hyperbolic geometry is characterized by an exponential growth of space as we move away from the center, mirroring the exponential growth of brain networks (Figure 1a). Building upon this insight, we designed a novel hyperbolic MEG brain network embedding framework that transforms high-dimensional complex MEG brain networks into lower-dimensional hyperbolic representations. Our approach involved the design and validation of a new hyperbolic model built upon the architecture of the fully hyperbolic neural network (FHNN). Using this model, we computed hyperbolic embeddings of the MEG brain networks of 587 individuals from the Cambridge Centre for Ageing and Neuroscience (Cam-CAN) dataset (Figure 1b). In addition, we included in the model anatomical features of cortical grey matter thickness and myelination (as obtained by magnetization transfer ratio). Notably, we introduced *a unique metric—the radius of the node embeddings—which effectively proxies the hierarchical organization of the brain*. We leveraged this metric to characterize subtle hierarchical organization changes of various brain subnetworks attributed to the aging process. Our findings revealed that a considerable number of subnetworks exhibit a reduction in hierarchy during aging, with some displaying gradual changes and others undergoing abrupt transformations in the elderly (examples in Figure 1cde). Overall, our study presents the first evaluation of hyperbolic embeddings in MEG brain networks, introduces a novel multi-modal measure of brain hierarchy, and uses this measure to highlight aging trajectories in the large cohort of the Cam-CAN dataset.

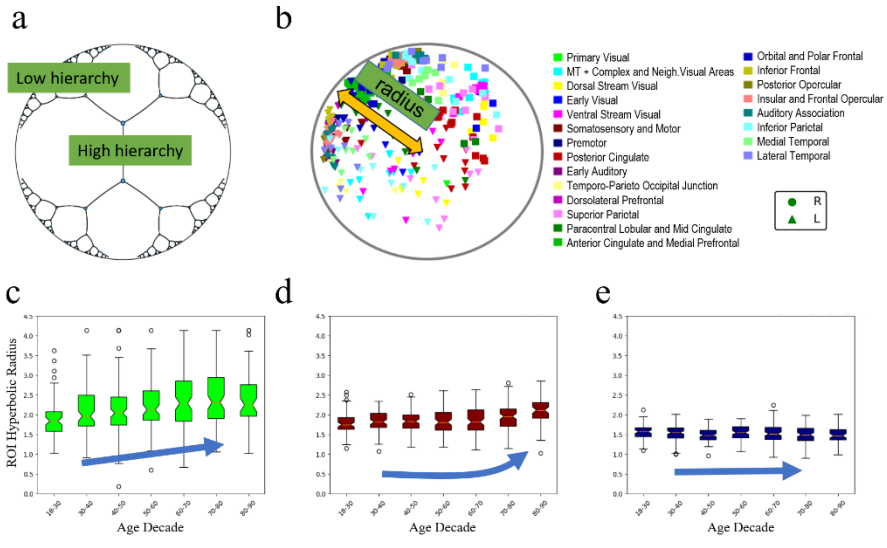


***Figure 1: Hyperbolic embeddings of brain networks reveal aging trajectories.*** *(a) Example hyperbolic embedding of a binary tree. Hyperbolic space expands exponentially from center due to its negative curvature, enabling embeddings with minimal distortion. (b) Example hyperbolic embedding of the MEG network of a Cam-CAN participant. The hyperbolic radius effectively proxies the hierarchical organization of the brain. (c-d-e) Hyperbolic radius of left primary visual cortex, right orbital and polar frontal, and left paracentral lobular and mid cingulate, respectively. Each ROI undergoes a different trajectory over decades.*

This work was supported by a J-Clinic for Machine Learning in Health at MIT grant award (to DP); and the National Institute on Aging of the National Institutes of Health under award numbers RF1AG074204 (to JCM, MF, FM, and DP) and RF1AG079324 (to EBM, JCM, MF, FM, and DP).

# The ENIGMA MEG resting state analysis pipeline

Jeff Stout[1], Anna Namyst[1], Allison Nugent[1]
1) National Institute of Mental Health, Bethesda MD

Introduction:
The ENIGMA consortium was initially created to investigate low powered genetic effects on hippocampal volume by combining MRI data across multiple sites. Building on this idea, the ENIGMA MEG working group was recently formed to combine MEG data across sites with over 30 participating labs across the globe. Compared with MRI analysis, additional complexity is present in cross-site MEG analysis because of inherent differences in vendor specific data formats, sensor geometries, noise levels, noise mitigation techniques and anatomical integration. The first project of this working group is to investigate source level spatial-spectral changes associated with age, gender, and patient populations. The ENIGMA MEG resting state pipeline is built on top of standard tools to read MEG BIDS format and process data into csv outputs in an automated fashion. As a proof of concept, the current analysis pipeline has been run on several major open access MEG datasets including: CAMCAN, MEGUK, MOUS, NIH HV, NIH MI, and OMEGA. Following validation of the pipeline on repository data, working group members can perform their analyses locally and provide anonymized csv results for meta-analysis.

Methods:
The ENIGMA MEG resting state pipeline uses MNE, MNE-BIDS, MEGNET, and FOOOF python packages to load, clean, localize activity to the brain and process source level spectral information. The T1w MRI scans were processed through Freesurfer to create a cortical reconstruction. The pipeline includes the following steps: [MRI] source space calculation, automated MEG/MRI coregistration including atlas based fiducial localization and minimum distance fit (if fiducial localizers are not included with the anatomical data), [MEG] 1-45Hz filtering, 300Hz downsampling, deep learning based MEGNET automatic ICA removal, epoching, noise/data covariance estimation, lcmv beamformer calculation, epoch projection, parcel data extraction, multi-taper power spectral density (PSD) estimation, and normalization by total spectral power. The FOOOF algorithm fits the 1/f background spectrum and oscillatory peaks compile results to a csv file. Group analysis is performed by merging the spectral outputs with the BIDS participants.tsv file and fitting a least squares regression.

Results:
The average time for data analysis (excluding cortical reconstruction) was approximately 30 minutes on a modern system with RAM usage between 2.5-5Gb depending on the size of the raw MEG data. As seen in figure 1, the compiled data demonstrated significant overlap with previously reported literature including the dominant anterior/posterior gradient of the alpha rhythm, known beta predominance in the somato-motor region, and anterior frontal and frontal midline theta peaks. This automated routine shows consistent and robust findings with minimal preprocessing effort.

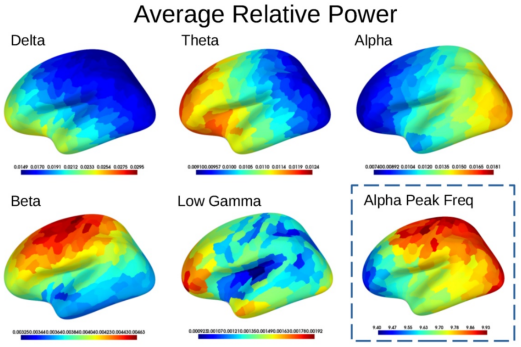


·Figure 1: Localized relative PSD averaged in standard frequency bands: Delta [1-3], Theta [3-6], Alpha [8-12], Beta [13-35], Low Gamma [35-45]. FOOOF fitted alpha peak in Hz plotted at each

Conclusions:
The ENIGMA MEG resting state pipeline is an easy to use open source codebase that has been used here to demonstrate consistent findings with previously published data. The ease of use allows automated data analysis that can be performed by typical MEG users without significant manual intervention. Future plans include incorporating data from the working group members and data harmonization for the following categories: site, hardware vendor, eyes open/closed, seated/supine. In summary the ENIGMA MEG resting state pipeline opens the doors for large scale cross-site analyses that will ultimately lead to more robust and reproducible findings.

Contrasting effects of anodal and cathodal high-definition TDCS on proprioceptive responses in sensorimotor cortex, measured with MEG during voluntary finger movements.

Jed A. Meltzer[1,2], Gayatri Sivaratnam[1], Tiffany Deschamps[1], Maryam Zadeh[1], Catherine Li[1], Alex Francois-Nienaber[1]

*[1]Rotman Research Institute, Baycrest Centre, Toronto, Canada [2]Department of Psychology, University of Toronto, Toronto, Canada*

Protocols for noninvasive brain such changes generalize to other cortical regions beyond motor cortex, and how such protocols might be expected to modulate stimulation (NIBS) are generally categorized as “excitatory” or “inhibitory” based on their ability to produce short-term modulation of motor-evoked potentials (MEPs) in peripheral muscles when applied to motor cortex. It is as yet poorly understood whether neural signals generated during task performance, at rest, or in response to sensory stimulation. To characterize such changes, we measured spontaneous and movement-related neural activity with magnetoencephalography (MEG) before and after high-definition transcranial direct-current stimulation (HD-TDCS) of the left motor cortex (M1), while participants performed simple finger movements with the left and right hands. Anodal HD-TDCS (aTDCS), thought to be excitatory, decreased the movement-related cortical fields (MRCF) localized to left M1 during contralateral right finger movements while cathodal HD-TDCS (cTDCS), thought to be inhibitory, increased them. In contrast, oscillatory signatures of voluntary motor output were not differentially affected by the two stimulation protocols, and tended to decrease in magnitude over the course of the experiment regardless. Spontaneous resting state oscillations were not affected either. Because MRCFs are thought to reflect reafferent proprioceptive input to motor cortex following movements, these results suggest that processing of incoming sensory information may be affected by TDCS in a polarity-dependent manner that is opposite that seen for MEPs – increases in cortical excitability as defined by MEPs may correspond to reduced responses to afferent input, and vice-versa.

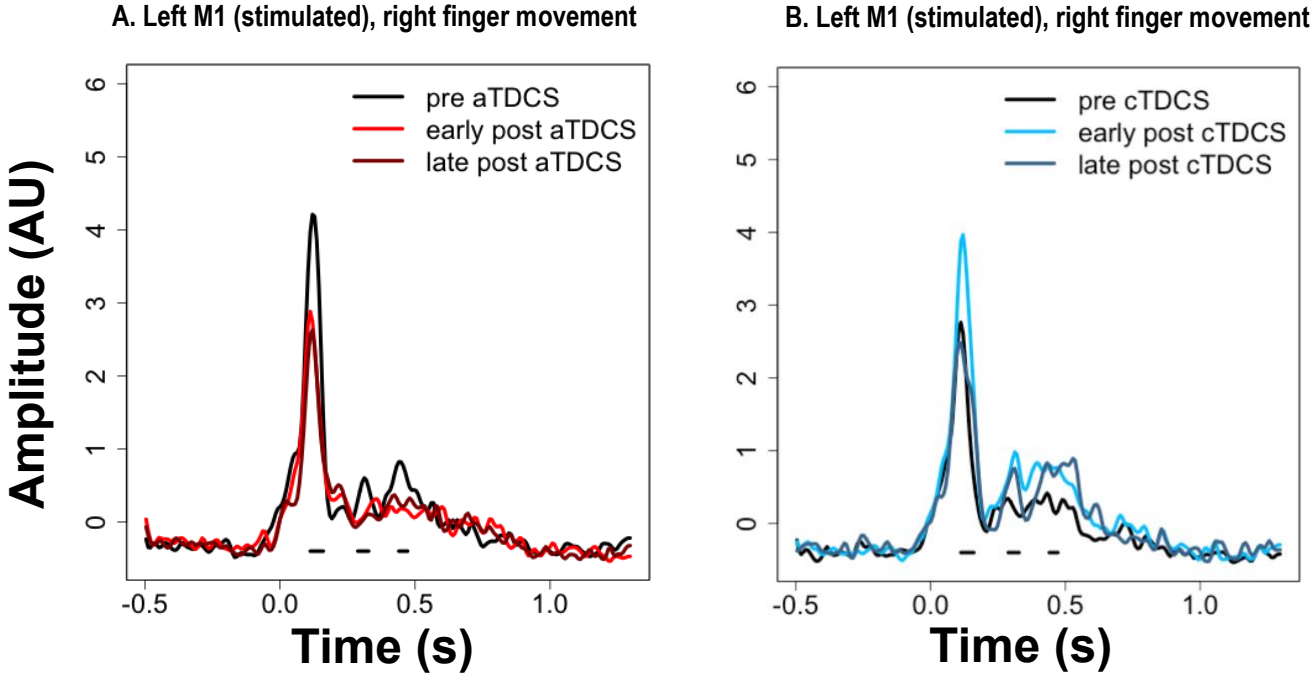

**Modulation of TMS-evoked transcallosal inhibition by voluntary hand movement**

Sabira Alibhai-Najarali

Purpose

Interhemispheric connectivity plays a key role in behavioural deficits in stroke and neurodegenerative disease, but a major debate questions whether homologous regions excite or inhibit each other. Linking inhibitory phenomena in the motor cortex to similar interactions in other cortical regions is a research imperative, and may be possible through measurements of electrophysiological connectivity using EEG or MEG. One promising signal is the post-movement-beta-rebound (PMBR), which is thought to reflect local inhibitory processing. In this study, we evaluate potential direct evidence for increased transcallosal inhibition occurring in the same period as PMBR, immediately following a voluntary movement.

Methods

We used the transcranial magnetic stimulation (TMS) paradigm called ipsilateral silent period (iSP), in which a unilateral hand squeeze is temporarily interrupted by a magnetic pulse to ipsilateral motor cortex, reflecting transcallosal inhibition of the contralateral motor cortex. Twenty, right-handed, participants were asked to make a button-press with the non-squeezing hand, which then triggered the TMS to randomly stimulate at 8 different time points, meant to overlap with the time course of PMBR. Additionally, to measure the time course of the PMBR, six different participants were asked to make the same button-press while their neural activity was measured with MEG.

Results

The extent of the iSP was not significantly modulated after voluntary movement in either the dominant or non-dominant hemisphere. Motor evoked potentials, reflecting excitability of the cortex controlling the voluntary movement, were increased 10 ms after movement offset but not at any subsequent timepoints. MEG recordings confirmed that the expected pattern of beta desynchronization and rebound was present for the button press movement.

Conclusion

Ipsilateral silent period does not appear to be significantly modulated following voluntary movement, suggesting that it does not share a common mechanism with the beta rebound observed in EEG and MEG recordings.

# Music-based fine motor rehabilitation in Parkinson's patients: feasibility, efficacy and neural correlates

[1]Isabelle Buard PhD, [1]Lucas Lattanzio BA, [1]Karrie Hardin, MMT MT-BC, [2]Michael Thaut PhD, [3]Benzi Kluger MD MS

1. University of Colorado Denver – Anschutz Medical Campus. Aurora, CO, USA
2. University of Toronto – Faculty of Music. Toronto, Canada
3. University of Rochester – Medical Center. Rochester, NY, USA

Objective: To assess the feasibility, preliminary efficacy and underlying mechanisms of a structured Neurologic Music Therapy (NMT) fine motor intervention in patients with Parkinson's disease (PD).

Background: Besides notable gross motor symptoms (e.g. bradykinesia, postural instability, etc…), fine motor impairments cause patients with PD difficulties everyday tasks such as writing, self-care, fine object manipulation, and therefore negatively impact their quality of life. NMT is an evidence-based clinical model consisting of standardized interventions using music for restorative training in neurorehabilitation. While NMT has provided benefit for gait in PD, possibly by mobilizing motor networks that have been spared during disease progression, its applicability within fine motor rehabilitation has not been explored yet. We hypothesized that NMT holds rehabilitative potential to improve fine motor abilities by increasing auditory-motor connectivity in the beta and gamma frequency bands.

Methods: We enrolled patients with PD to undergo a structured 5-week course of NMT emphasized on fine motor training (Buard et al., 2021). Study participants were evaluated in person to collect assessments prior to starting NMT, and after cessation of therapy. Outcome measures included: (i) Unified Parkinson's Disease Rating Scale (UPDRS) (ii) Grooved Pegboard Test (GPT) scores and (iii) Magnetoencephalography (MEG).

Results: Sixty participants with PD (11 withdrawals) were enrolled in the study. Our control group included twenty-one patients with PD. From all those who completed the study, adherence and compliance to the NMT intervention was 100%. NMT improved PD motor symptoms, with a 13.4% and 22.4% respective reduction (greater scores are associated with greater motor symptoms) in dominant and non-dominant hand motor scores. Fine motor dexterity was also improved: ANOVA followed by pairwise comparisons indicated a significant increase in dominant hand dexterity ($p=0.026$) but not in the non-dominant hand ($p>0.05$) compared to those in the waitlist group. Last, MEG results on a sub cohort indicated an increased beta evoked power in the motor cortex after NMT, an increased functional connectivity between the auditory and motor regions and a distinct neurophysiological profile for the high vs. non responders to the NMT intervention.

Conclusions: We suggest that using music-based fine motor rehabilitation for patients with PD is not only feasible but also holds great promise for enhancing fine motor skills by influencing cortical patterns. Furthermore, the varying responses among individuals and the neurophysiological differences among them present an opportunity to customize music therapies specifically for PD patients. However, due to the limited number of participants in our study, we believe it is essential to conduct further research in this area. Last, using MEG could deepen our understanding of the neuropathophysiology associated with these diseases and shed light on the mechanisms behind successful NMT interventions for upper extremity rehabilitation.

**Title:** Magnetoencephalographic Correlates of Reward Processing in Mood Disorders

**Authors:** Amy Xu[1], Elizabeth D. Ballard, Ph.D., Carlos Zarate Jr.[1] M.D., Jessica Gilbert[1] Ph.D.
[1]Experimental Therapeutics and Pathophysiology Branch, National Institute of Mental Health, Bethesda, MD

**Abstract:**

Background

Ketamine has been identified as a promising, rapid-acting antidepressant, but its neural mechanism of action is still poorly understood. Previous research has suggested that its impact on reward processing circuitry may play a role in its antidepressant effect, though there have been conflicting reports on how it impacts behavioral aspects of reward processing. In this study, participants with a mood disorder (MD) and healthy controls (HC) completed a modified version of the Monetary Incentive Delay Task (MID) during a magnetoencephalography (MEG) scan. A subsample of the MD group completed a second scan either during (MD-Ket) or one day following (MD-KDB) an intravenous subanesthetic ketamine infusion (0.5 mg/kg). In this preliminary analysis of the MD sample, behavioral data (accuracy and reaction time, RT) was examined. Based on previous literature, it was predicted that ketamine would alter reward-related processing of monetary gains and losses in MD participants.

Methods

Twenty-six participants (23 MD, 3 HC) completed the MID task. In addition, within the MD sample, 12 participants received ketamine (5 MD-Ket and 7 MD-KDB). MEG data was recorded using a CTF 275 MEG system. In each session, accuracy was calculated and compared at baseline and following ketamine for monetary gain and loss trials. Bias scores were calculated by subtracting RT for loss trials from gain trials to compare reward-related biases at baseline and following ketamine, to control for acute drug effects on RT.

Results

Within the MD sample, there was a significant increase in accuracy for gain trials from baseline (66.8%) to ketamine (75.9%) ($t=-2.6$, $p<0.05$) and no difference in the accuracy of loss trials from baseline (64.7%) to ketamine (69.7%). In addition, there was a significant increase in RT bias from baseline (-2.8) to ketamine (-14.6) ($t=2.4$, $p>0.05$), reflecting faster reaction times to gains versus losses following ketamine.

Discussion

These findings suggest that ketamine alters reward-related behavior in MDs by motivating individuals towards gains over losses. Planned analyses will examine the effects of gain and loss trials on gamma power (a proxy measure of excitation-inhibition balance) for both MD and HC participants, in addition to examining the effect of ketamine on gamma power and anhedonia in the context of reward-related processes.

**Funding Source:** Intramural Research Program at the National Institute of Mental Health, National Institutes of Health

**Keywords:** reward processing, magnetoencephalography, mood disorders, ketamine

**Title:** Phenotype of frontal lobe glioma determines the frequency band specific functional connectivity alteration.

**Authors:** Apisit Kaewsanit[1,2,3], Velmurugan Jayabal[1], Leighton Hinkley[1], Kiwamu Kudo[4], Gavin Belok[1], Mahmoud Jiha[1], Joshua Chon[1], Dylan Davis[1], Srivatsan Tennathur[1], Anne Findlay[1], Corby Dale[1], Heidi E. Kirsch[1], Mitch Berger[5], Shawn Hervey-Jumper[5], and Srikantan S. Nagarajan[1]

**Abstract: Background:** Highly prevalent frontal lobe glioma is associated with pathologically high brain activity, which relates to rapid progression. Regional and whole brain functional connectivity is altered in these patients impacting the treatment and the survival of these patients. Molecular characteristics, such as isocitrate dehydrogenase (IDH) mutations and 1p/19q codeletion, are proved to be survival deterministic biomarkers. We investigated the whole brain functional connectivity of frontal glioma in IDH-wild and IDH-mutant type tumors and their relationship with the disease progression. **Methods:** We evaluated 150 patients with frontal lobe glioma from the UCSF medical center who completed presurgical magnetoencephalography during 2011 to 2022. All these patients underwent surgery and their histopathological and molecular findings were noted. Each participant underwent a 10 minute resting-state MEG at the UCSF Biomagnetic Imaging Laboratory. For each patient, the voxel-level brain source time series was computed using adaptive spatial filters at a resolution of 10mm. Subsequently, functional connectivity was computed using imaginary coherence after parcellating the voxels into 246 brain regions using brainnetome atlas. Such interactions were evaluated at 5 different frequency bands including delta (1-4Hz), theta(4-8Hz), alpha(8-12Hz), beta(12-30Hz), and gamma(30-70Hz). Within and between group non-parametric statistical tests were computed at the ROI level ($p<0.05$) after correcting for multiple comparisons with permutations testing. **Results:** This study included 150 patients (male=60.7%; age=50.7±14.8) diagnosed with frontal lobe glioma (hemisphere left -77 and right-73). The most common integrated diagnosis was glioblastoma with IDH-wildtype in 72 patients (48%) and IDH-mutant in 78 patients (52%). Regardless of the type of tumor, all these patients consistently show pathologically increased whole brain connectivity particularly in the lower frequency bands (delta, theta and alpha). IDH-wildtype tumors have substantially increased connectivity specifically during delta and beta frequency bands when compared with mutant type tumors; on the contrary, IDH-mutant tumors have increased connectivity in the theta and alpha frequency bands when compared with wild type. We observed statistically significant differences in the distribution of connectivity patterns between the IDH-mutant and IDH-wildtype groups in all the frequency bands except the gamma band. Frontal and insular regions showed relatively decreased clustering coefficient compared to the other regions of the brain. **Conclusion:** Patients with frontal gliomas exhibit a frequency band specific alterations in the connectivity and low network clustering. This study might provide insight into our understanding of the aggressive nature of the tumor and its progression with prognostication.

**Author affiliations:**
1Biomagnetic Imaging Laboratory, Department of Radiology and Biomedical Imaging, University of California, San Francisco, CA, 94143, USA
2Training in Clinical Research Graduate Programs, Department of Epidemiology and Biostatistics, University of California, San Francisco, CA, 94158, USA
3Department of Anatomy, Phramongkutklao College of Medicine, Bangkok, 10400, Thailand
4Medical Imaging Business Center, Ricoh Company, Ltd., Kanazawa, 920-0177, Japan
5Department of Neurological Surgery, University of California, San Francisco, CA, 94143, USA

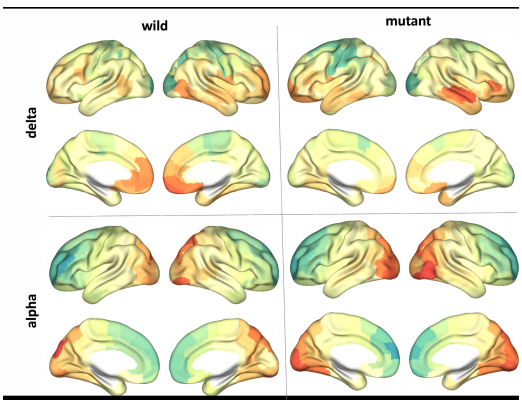


Figure-1: This figure illustrates the regional level connectivity differences in the delta and alpha frequency band of the wild and mutant phenotype of frontal gliomas.

# ASD and TD individuals show increased cortical responses to shift in sound source during a spatial hearing task

Sergio Osorio[1,2], Jasmine Tan[1,2], Grace Levine[1,2], Seppo P Ahlfors[1,2], Steven Graham[2], Fahimeh Mamashli[1,2,3], Sheraz Khan[1,3], Robert M Joseph[4], Ainsley Losh[2], Stephanie Pawlyszyn[2], Nicole McGuiggan[2], Matti S Hämäläinen[1,3], Hari Bharadwaj[5,6], Tal Kenet[1,2`]

[1] Athinoula A. Martinos Center for Biomedical Imaging, Massachusetts General Hospital, Charlestown, MA, USA
[2] Department of Neurology, Harvard Medical School, Massachusetts General Hospital, Boston, MA, USA
[3] Department of Radiology, Harvard Medical School, Massachusetts General Hospital, Boston, MA, USA
[4] Department of Anatomy and Neurobiology, Boston University School of Medicine, Boston, MA, USA
[5] Department of Communication Science and Disorders, University of Pittsburgh, Pittsburgh, PA, USA
[6] Department of Speech, Language, and Hearing Sciences, Purdue University, West Lafayette, IN, USA

Abnormalities in auditory processing have been documented across a wide range of stimuli in individuals with autism spectrum disorder (ASD). However, relatively few studies have investigated spatial hearing in ASD. Spatial hearing, i.e., the correct localization of sound sources and ability to track changes in location is a critical component of social interactions, and therefore merits further attention. Here, we investigated MEG responses in ASD (n = 21, mean = 13.55, SD = 2.69) and TD (n=28, mean = 13.07, SD = 3.43) to ~1000ms to auditory stimuli presented to either left or right ear (*stay* condition) vs stimuli shifting to the contralateral ear at ~550ms (*jump* condition), where the "stay" condition corresponds to no change in auditory source location, whereas the "jump" condition corresponds to a perceived change in source location. sLORETA source modeling was used to extract responses from subject-specific labels within cortical temporal regions corresponding to the peak activation to jump events. Preliminary results show evoked responses aligned with the onset of sound shift with an average peak at around 750ms in right (TD: mean latency = 754ms, SD = 0.033) and left (TD: mean latency = 750ms, SD = 0.029) hemispheres for the TD group. For both groups, activation was higher for jump relative to stay events in left hemisphere ($TD_{jump}$: mean = 4.05, SD = 2.06 vs. $TD_{stay}$: mean = 3.24, SD = 1.69; $ASD_{jump}$: mean = 3.51, SD = 1.14 vs. $ASD_{stay}$: mean = 3.00, SD = 1.75) versus right ($TD_{jump}$: mean = 4.13, SD = 2.25 vs $TD_{stay}$: mean = 2.43, SD =2.11; $ASD_{jump}$: mean = 4.08, SD = 2.03 vs. $ASD_{stay}$: mean = 2.95, SD = 2.18). A linear mixed effect model for group, hemisphere and condition as fixed effects and subject and group as random intercepts shows a significant contribution of condition (*stay*: b = -0.68, p = 0.028, SE = 0.31) in predicting lower amplitude cortical responses, but no significant effect for group, hemisphere, or the group-by-hemisphere and group-by-condition interactions. While no differences were observed across groups, most likely due to very high observed variability, qualitative differences in early-latency negative deflections and ASD-specific latencies for activation peaks that might reveal more subtle across-group differences.

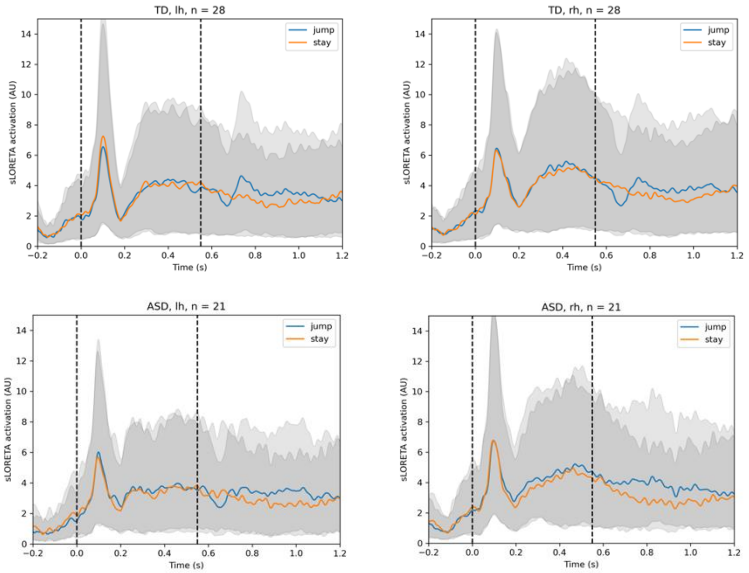

# The Balance Between Top-Down and Bottom-Up Attention in Misophonia

Jasmine Tan[1,2], Sergio Osorio[1,2], Grace Levine[1,2], Seppo P Ahlfors[2,3], Julie Arenberg[4], Tal Kenet[1,2]

*[1]Department of Neurology, Massachusetts General Hospital and Harvard Medical School, Boston, MA, United States*

*[2]Athinoula A. Martinos Center for Biomedical Imaging, Massachusetts General Hospital, Charlestown, MA, United States*

*[3]Department of Radiology, Massachusetts General Hospital and Harvard Medical School, Boston, MA, United States*

*[4]Department of Audiology, Massachusetts Eye and Ear and Harvard Medical School, Boston, MA, United States*

Misophonia is a disorder of abnormal emotional reactions to specific sensory stimuli, and in particular auditory stimuli. While mechanisms involving differential reactivity of emotional regulation, learning and auditory processing have been proposed, thus far little is known or understood about the neural basis of misophonia.

Auditory sensitivities are also commonly associated with autism spectrum disorder (ASD). We have previously shown that abnormal sensory processing in ASD has been is linked to abnormally increased bottom-up cortical functional connectivity. At the same time, there is evidence that top-down processes that would typically down-regulate cortical responses to stimuli are reduced in ASD.

Since abnormal sensory reactivity in misophonia is stimuli-specific, rather than generalized, as is the case most often in ASD, we hypothesize that participants with misophonia will show increased top-down functional connectivity from cortical areas that modulate attention into the auditory cortex. We further hypothesize that unlike ASD participants, they will only show this increased functional connectivity during aversive triggering auditory stimuli, indicating that misophonia is top-down regulated.

To test this hypothesis, we are using magnetoencephalography (MEG) to measure bottom-up and top-down functional connectivity during an auditory spatial attention task. Participants are instructed to perform a classic auditory oddball paradigm while attending to only to the cued ear. Attention to the deviant tone in the attended ear is driven by “top-down” attention, which is voluntary and spatially specific. Participants are also instructed to ignore sounds in the non-cued ear, which will involve novel stimuli such as claps or clinks, as well as sounds that are specially selected to trigger misophonia in each individual participant, such as chewing. While all distractor sounds will elicit involuntary “bottom-up” attention, we expect that in misophonia participants, the misophonia-specific sounds will also trigger greater than expected top-down processes.

Data collection is ongoing. Preliminary analyses of our first two participants show that in comparison to the neurotypical participant, the participant with misophonia shows larger differences between evoked responses to misophonic triggers versus non-misophonic triggers. Further analyses with additional participants will examine functional connectivity to test our hypotheses.

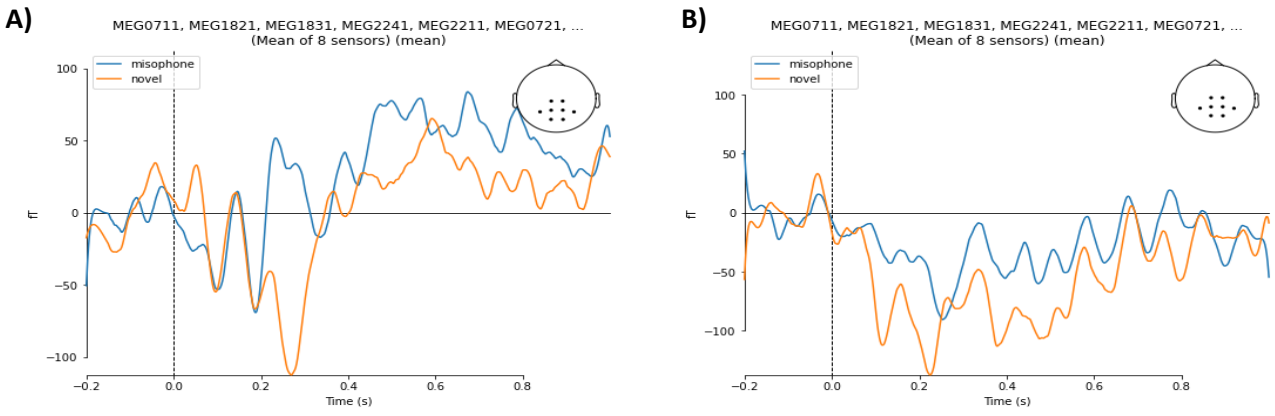


*Figure 1 Example evoked responses from central sensors from A) a misophonic participant and B) a neurotypical participant. Between 200ms to 400ms after the sound is presented, the misophonic participant shows a positive peak in the central area to the misophonia-triggering sound but a negative peak to the novel, non-triggering sound. The neurotypical participant shows a similar response to both the misophonia-triggering sound and the non-triggering sound.*

**Title**: Novel clinical MEG/MSI approach to detect and localize the subtle and non-localizing epileptogenic events.

Velmurugan Jayabal, Heidi Kirsch, Anne Findlay, Mahmoud Jiha, Dylan Davis, Srivatsan Tennathur, Gavin Belok, Joshua Chon, Mary Mantle, Heidi Kirsch, Srikantan Nagarajan

**Department of Radiology and Biomedical imaging, University of California San Francisco (UCSF)*

**Background:** MEG is used in phase-1 evaluation of refractory epilepsy patients to delineate the epileptogenic foci. There are circumstances where identifying interictal epileptiform discharges (IEDs) in the raw data can be challenging, and or the standard single dipole fitting method may fall short in modeling some of these epileptogenic events. Here we propose a strategy to identify the interictal events and subsequently localize or map their source generators. **Methods:** We prospectively applied this strategy in 23 patients during our first clinical MEG meeting, when there was a concern or difficulty with the detection or localization using traditional equivalent current dipole fitting method. The effectiveness of this approach was evaluated on different levels, including Level I: Consistent agreement with the standard dipole fitting approach findings; Level II: Able to identify events that is not detectable in the raw data; Level III: inability of employing standardized methods to localize the source of non-localizing events. The recorded MEG data was analyzed with a unique strategy (Velmurugan et al 2022) by combining the spatial filter (minimum variance adaptive beamformer) and a blind source separation (independent component analysis-ICA). The resulting source components were then reviewed manually for the presence of IED on the basis of their electrophysiological characteristics and morphology. Presumed epileptogenic zone (EZ) was estimated for each patient based on their pre-surgical electrophysiological (EEG and video telemetry) and neuroimaging (MRI/PET/SPECT) studies. We evaluated the concordance between presumed EZ and the source localization results obtained using our approach. **Results:** MEG data was reviewed for distinct spikes, polyspikes, sharp waves, beta bursts, ictal-interictal continuum and rhythmic focal slowing amidst the background activity. The current approach detected additional interictal events that were not detected during the conventional MEG data review in 6 patients (26%) at the level 2. Non-localizing and subtle events identified during conventional clinical analysis were able to successfully localize in 11 patients (48%) at the level 3. In another 6 patients (26%), obtained results agreed to the conventional ECD modeling at the level 1 agreement. In 76% of the patients (n=19), more interictal episodes were detected utilizing our method than during the traditional review. The source localization results generated using the suggested technique demonstrated a substantial spatial concordance with the assumed EZ (Cohen's k =0.79). Our approach provided insight and assisted in the challenging clinical interpretation especially in the following EZ regions: mesial frontal and deep sources such as cingulate, insular,sulcal depth, mesial temporal sources, multifocal epilepsies and bitemporal epilepsies (Figure-1).**Conclusion:** This analytical strategy intends to enhance the IED detection and localization accuracy of the epileptogenic zone. Additionally, it minimizes the arbitrary bias of choosing interictal spikes and determining a time interval to simulate the dipole fit.

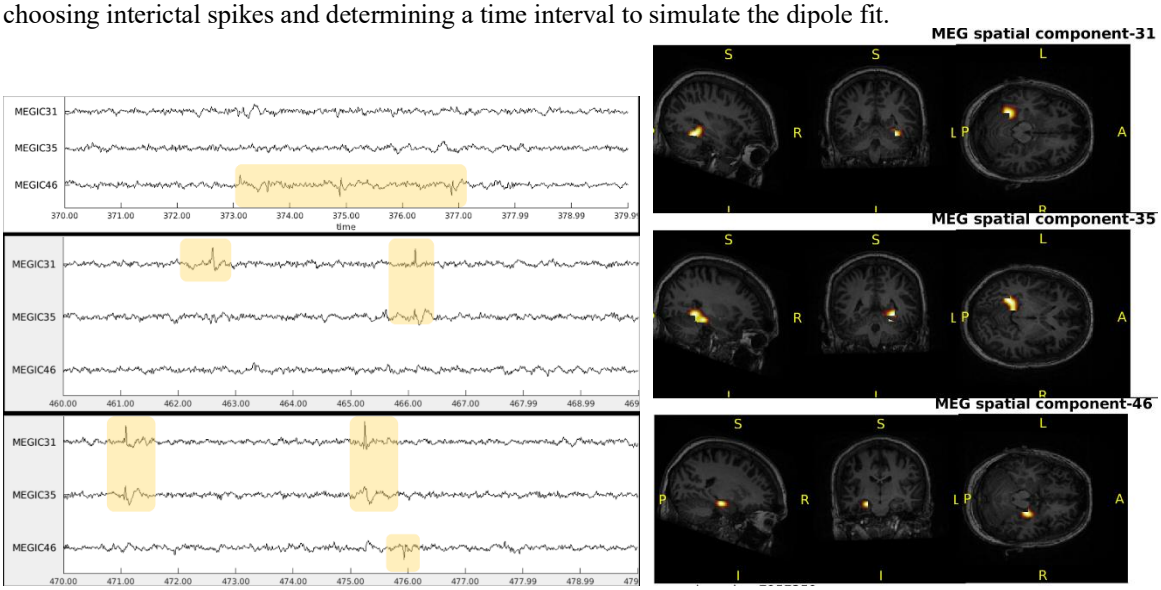


**Figure-1:** *This figure illustrates a patient with bi-temporal focal cortical dysplasia where routine EEG and MEG reading picked up only the left temporal spikes and sharp waves (MEG IC-31 and 35). However, with the proposed approach we were able to detect the asynchronous low amplitude spikes and sharp waves in the right mesial temporal lobe which is consistent with this patient's presumed epileptogenic zone.*

**Title: Advanced MEG Data Processing in Epilepsy Patients with RNS**

**Authors:** Pegah Askari, Natascha Cardoso da Fonseca, Tyrell Pruitt, Joseph A Maldjian, Sasha Alick-Lindstrom, Elizabeth M Davenport

**Affiliation:** The University of Texas Southwestern Medical Center, Dallas, USA

**Introduction:** The RNS® System is an FDA-approved implantable responsive neurostimulator for treating drug-resistant focal epilepsy (DRE). Its effectiveness is well documented; however, some patients may undergo additional tests to inform a further surgical intervention. Magnetoencephalography (MEG) is a valuable FDA-approved tool for evaluation of DRE. The cranially implanted RNS neurostimulator generates electric/magnetic fields that may interfere with MEG recordings. This study aims to test advanced signal processing methods to improve clinical utility of MEG recordings in patients with an RNS neurostimulator and leads.

**Methods:** Clinical resting-state MEG scans were performed using a 306-channel MEGIN Triux-Neo for two epilepsy patients (Subject 1: F, 42y/o; Subject 2: M, 32y/o) treated with the RNS Systems. We recorded data in two modes: (1) with stimulation disabled but detection and storage enabled (MRI mode) and (2) with stimulation, detection, and storage disabled (off mode). Conventional pre-processing, temporal signal space separation (tSSS), was performed on raw data. MEG sensor level data was then further pre-processed using MNE-Python. This advanced processing method included a band-pass filter of 1-70Hz, an independent component analysis (ICA), and automated removal of electrooculogram (EOG) and electrocardiogram (ECG) artifact components. The power spectral density (PSD) was computed for all channels using Welch's method for both conventional and advanced processing methods. The PSD from all channels was used to calculate the average signal-to-noise (SNR) ratio of the advanced processing to conventional processing. SNR was also calculated for both processing methods comparing channels directly above the RNS and channels on the contralateral hemisphere with less RNS interference.

**Results:** The SNR values from the RNS System in MRI mode have not been reported due to extremely limited MEG recording quality, possibly due to the increased electrical activity associated with the detection and storage functions. The SNR values in off mode are shown in Table 1. Negative SNR values imply that the noise is much greater than the signal, particularly in sensors above the neurostimulator. A board-certified epileptologist qualitatively confirmed improved readability of the signals after advanced processing.

**Table 1.** The results from SNR calculations (mean ± Standard deviation SD in decibels dB).

| | Subject 1 SNR | Subject 2 SNR |
|---|---|---|
| RNS mode OFF (Conventional vs. Advanced (Average of All Channels)) | 0.14±0.75 | -0.61±0.78 |
| RNS mode OFF (RNS Channel vs. No RNS using Conventional method) | -18.49± 1.20 | -18.22±1.90 |
| RNS mode OFF (RNS Channel vs. No RNS using Advanced method) | -16.89±0.35 | -15.66±1.07 |

**Conclusions:** MEG data with the RNS System yielded clinically viable data when the RNS was in off mode. Utilizing advanced signal processing, we were able to significantly improve the SNR as well as readability of the MEG data. However, the SNR in channels directly over the neurostimulator is still poor and may require modified MEG acquisition methods or strategic neurostimulator placement. Future work will compare MEG dipoles from both methods to SEEG and surgical outcomes.

**Altered gamma power oscillations in patients with comorbid temporal lobe epilepsy and psychiatric disorders: a novel MEG spectral analysis.**

**Natascha Cardoso da Fonseca[1,2], Amy Proskovec[1,2], Sasha Alick-Lindstrom[1,3], Chadrick Lane[4,5], Joseph Maldjian[1,2], Elizabeth Davenport[1,2]**

[1]MEG Center of Excellence, Department of Radiology, UTSW Medical Center; [2]Advanced Neuroscience Imaging Research (ANSIR) laboratory, Department of Radiology, UTSW Medical Center; [3]Department of Neurology, UTSW Medical Center; [4]Department of Psychiatry, Peter O'Donnell Brain Institute; [5]UTSW Medical School

**Introduction:** Temporal lobe epilepsy (TLE) shares a well-established and significant connection with psychiatric disorders (PD). PD in TLE is correlated with reduced response to pharmacological and surgical treatments and a decline in quality of life. Hence, recognizing and addressing it is imperative. We performed a novel MEG spectral analysis in TLE patients to investigate the relationship between gamma oscillations and PD. **Methods:** Resting-state MEG data from 25 drug-resistant TLE patients, 17 with comorbid anxiety or depression, were used. Time-frequency decomposition in source space and a permutation t-test were performed between TLE patients with and without PD (Figure 1). Low gamma power maps were exported and compared between groups in Graph Pad, assuming significance $\alpha = 0.05$ (Figure 2). **Results:** Low gamma power was significantly increased in the frontal and cingulate regions and decreased in the occipital regions of patients with PD compared to the control group. Analyzing ROIs implicated in the default mode network (DMN), there was an increase in gamma in the PD group's medial prefrontal cortex, posterior cingulate, and precuneus compared to the control. Low gamma power was not associated with epilepsy duration or age (Pearson test, $p = 0.76$ and $p = 0.80$, respectively). **Conclusions:** Previous EEG studies have demonstrated the role of gamma oscillations in PD. Nevertheless, this is the first study demonstrating that gamma oscillations are also altered in patients with PD and comorbid epilepsy, including regions associated with the default mode network. While further evaluation is necessary, our findings corroborate the role of gamma oscillations as a potential neuroimaging biomarker for PD.

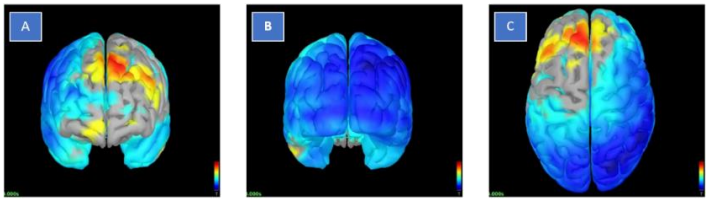


**Figure 1**. A, B, and C. 3D brain image of a template brain in anterior (A), posterior (B), and superior views (C) evidencing the results of the permutation t-test with false-discovery rate correction of low gamma band in TLE patients with PD compared with TLE without PD, performed in Brainstorm software. The areas in yellow and red (higher) evidence significantly increased gamma power, and the areas in light and profound (lower) blue evidence a significant decrease in gamma power. A. Anterior view, B) Posterior view, C) Superior view.

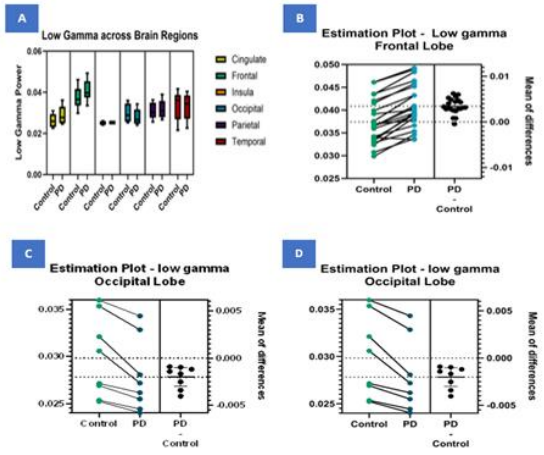


**Figure 2.** Graphs: A. Boxplot evidencing the mean low gamma power across regions in TLE patients with and without PD. B, C, D. Estimation plots evidencing the results of the unpaired t-test between TLE patients with and without PD in the frontal (A), cingulate (B), and occipital (D) regions of interest.

**MEG and Repetitive Head Impact Exposure in Youth Football Players**

Authors: Natalie M. Bell[1*], Fang F. Yu[1], Yin Xi[1], Jillian E. Urban[2], Amy Proskovec[1], Chris T. Whitlow[2], Joel D. Stitzel[2], Joseph A. Maldjian[1], Elizabeth M. Davenport[1]

The University of Texas at Southwestern Medical Center[1], Wake Forest University School of Medicine[2]

**Objective:** The objective of the present analysis was to compare imaging variables between a control group and groups of players with the highest and lowest head acceleration scores throughout the season.

**Materials and Methods:** 72 youth football players (all male; average age = 12.2 y) and 17 non-contact sport controls (all male; average age=11.5y) were included in this study. Football players wore sensor-embedded helmets that measured head impacts throughout the season. From this data, rotational and linear risk-weighted exposure (RWE) measures were calculated per subject. Control participants were assumed to have a 0 RWE value. In addition to the control group, four groups of 17 football players each were created with this data: lowest rotational RWE (L-$RWE_{Rotational}$), lowest linear RWE (L-$RWE_{Linear}$), highest rotational RWE (H-$RWE_{Rotational}$), and highest linear RWE (H-$RWE_{Linear}$). DKI MRI and 8-minutes of eyes-open resting-state MEG data were acquired pre-season and post-season. MEG data underwent standard pre-processing, and the images were source localized to the structural T1w MRI in Brainstorm. The relative power per frequency band and mean kurtosis (MK) for each voxel were calculated and normalized to MNI space. Voxel-wise difference maps (post-season minus pre-season) were computed for each frequency band per subject. Voxel-wise z-scores were computed utilizing the control group's mean and standard deviation. Whole-brain z-score maps were thresholded at 2 standard deviations above the mean of the controls resulting in the number of abnormal voxels (AV) per imaging measure. To identify significant differences between groups and to pinpoint the imaging variable that could best differentiate the highest head impacts from the lowest and control groups, we conducted a two-step analysis consisting of a multivariate analysis of covariance (MANCOVA) followed by a linear discriminant analysis (LDA).

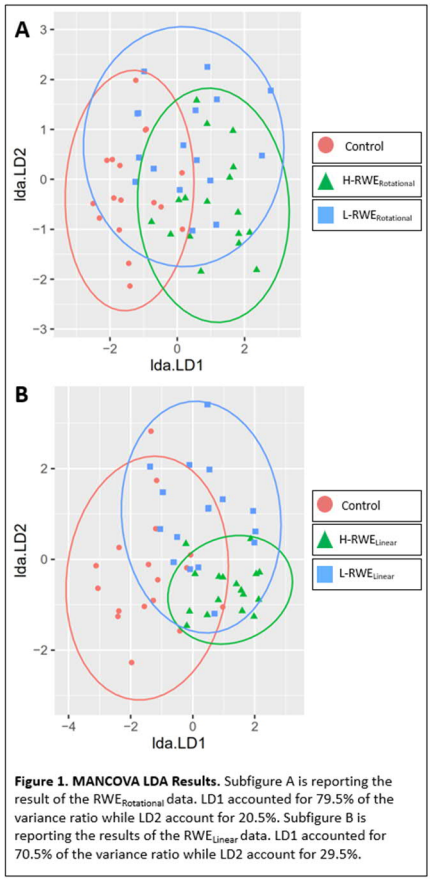


**Figure 1. MANCOVA LDA Results.** Subfigure A is reporting the result of the $RWE_{Rotational}$ data. LD1 accounted for 79.5% of the variance ratio while LD2 account for 20.5%. Subfigure B is reporting the results of the $RWE_{Linear}$ data. LD1 accounted for 70.5% of the variance ratio while LD2 account for 29.5%.

**Results and Discussion:** When evaluating between football player (H-$RWE_{Rotational}$ and L- $RWE_{Rotational}$) and control groups, the MANCOVA model was significant ($p<0.05$) and the model's effect size was 0.27. A LDA analysis looks at Fisher's linear discriminants LD1 and LD2. Firstly, LD1 is representative of a linear function that achieves the maximum separation between groups and identifies the variable(s) responsible for this differentiation, while LD2 is a linear function orthogonal to LD1 that also identifies the variable(s) responsible for maximal differentiation between all three groups. The LD1 results demonstrated higher AV in theta and MK differentiated the H-$RWE_{Rotational}$ group from the other groups, while LD2 indicated lower theta values differentiated L- $RWE_{Rotational}$ football players and control groups. A lower AV in low gamma differentiated the controls from the other groups. When comparing the results between the football players (H-$RWE_{Linear}$ and L-$RWE_{Linear}$) and control groups, the MANCOVA model was significant ($p<0.0001$) and the model's effect size was 0.42. The LD1 results demonstrated higher AV in MK differentiated all football players from the control group, while LD2 indicated that lower AV in theta differentiated H-$RWE_{Linear}$ from L-$RWE_{Linear}$ football players and controls.

**Conclusions:** In conclusion, our analysis indicated that MEG and DKI can be valuable tools for monitoring the progression of RSHI in pediatric populations. Specifically, we demonstrated that MK was able to distinguish controls from football players, while theta differentiated the high RSHI exposure group from the lowest RSHI exposure group and controls.

# Temporal signatures of multidimensional object properties in the human brain

Lina Teichmann[1], Martin N. Hebart[1,2,3], Chris I. Baker[1]

Our visual world consists of a huge variety of objects and yet we effortlessly identify, distinguish, interact, and reason about the things we see. This ability requires flexibility to integrate and focus on different object properties to enable diverse behavioral goals. What neural mechanisms support such a challenging task in the span of just a few hundred milliseconds? To address this question, we combined time-resolved MEG signals evoked by viewing thousands of objects with behavioral embeddings (Figure 1A). Specifically, we used millions of crowdsourced similarity judgments to model the neural representation of the object space and examined temporal profiles across behaviorally-relevant object dimensions. Overall, we found that the response to object properties in general starts to emerge at ~90 ms after stimulus onset and is initially driven by posterior sensors before it becomes more distributed at ~300 ms (Figure 1B). Looking at individual timecourses (Figure 1B rose plots & Figure 1C), we identified distinct temporal profiles for different dimensions. These profiles fall into two broad categories, with either a distinct and early peak (~150 ms) or a slow rise to a late peak (~300 ms). Further, the early effects are stable across participants, in contrast to later effects which show more variability across people. This highlights that early peaks may carry stimulus-specific and later peaks subject-specific object information. Given that the dimensions with early peaks seem to be primarily visual dimensions (e.g., white, colorful, cylindrical) and those with later peaks more conceptual (e.g., food-related, transportation-related), our results suggest that conceptual processing is more variable across people. Together, these data provide a comprehensive account of how the representation of object properties unfolds in the human brain.

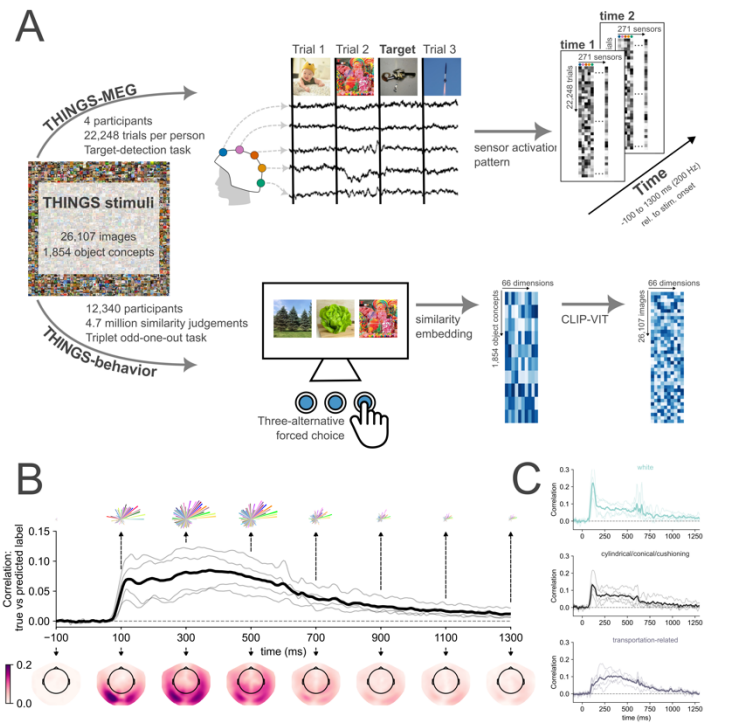


*Figure 1. (A) Dataset description for MEG and behavioral data. (B) Time-resolved information across all object dimensions in the signal, with rose plots showing single dimension activations at certain timepoints. (C) Selected temporal profiles for three dimensions highlighting variability in temporal structure.*

[1]Laboratory of Brain and Cognition, National Institute of Mental Health, National Institutes of Health, Bethesda MD, USA
[2]Vision and Computational Cognition Group, Max Planck Institute for Human Cognitive and Brain Sciences, Leipzig, Germany
[3]Department of Medicine, Justus Liebig University, Giessen, Germany

# Decoding Individual sequence skill learning actions during planning and execution

**Debadatta Dash,** Fumiaki Iwane, Roberto Salamanca-Giron, Marlene Bonstrup, Ethan Buch, Leonardo Cohen
HCPS, NINDS, NIH

Background: Activities of daily living rely on our ability to learn new skills composed of precise action sequences. Deconstructing a sequence and decoding individual actions is challenging, since both the individual action and precise role of the action within the sequence are simultaneously represented by ongoing neural activity dynamics. Furthermore, while the representations of individual actions are known to be stationary, representation elements related to sequence structure are likely to evolve over time. This study attempts to address this problem by decoding the neural representation of sequence-dependent individual actions during skill learning for improved decoding performance. Accurate decoding performance is important in detection of neural replay events – important markers for investigating memory formation and consolidation – as well as in applications of rehabilitation-oriented brain-machine interfaces (BMIs).

Methods: We recorded magnetoencephalography (MEG) recordings of 26 participants while they learned to perform a novel motor skill (typing [4 (index) – 1 (little) – 3 (middle) -2 (ring) – 4 (index)]) with their non-dominant left hand over 36 trials of practice (10 s) interspersed with rest (10 s) (Fig.1). We trained machine learning decoders to classify individual finger movements from neural oscillatory activity measured in source space. We then evaluated the decoding performance for each trial and related to the trial-by-trial behavioral performance defined as correct sequence typing speed (skill). Additionally, we examined trial-by-trial changes in the neural representation of the same (index) finger movement at different ordinal positions of the sequence in relation to skill over rest (micro-offline: Between trials) and practice (micro-online: within trial) periods within the training session.

Results: Finger identities were successfully decoded preceding movement onset (~86% accuracy) and during movement execution (~90% accuracy). Low frequency oscillations (LFO, delta: 1-3 Hz and theta: 4-7 Hz) in superior frontal, pre- and post-central, and middle frontal regions contributed the most to decoding (Fig.2). Optimal decoding performance was obtained using a hybrid combination of whole brain parcels and the voxels of these motor networks. Decoding accuracy improved progressively tracking performance gains during early learning (initial 11 trials where performance reached to 95% of peak performance) and plateaued when performance stabilized during late learning (12- 36 trials). The neural representations of the index finger at different ordinal positions of the sequence differentiated progressively during early learning. This differentiated representation correlated strongly with skill gains ($r$ = -0.868, $R^2$ = 0.753, $p$ < 0.001) and developed predominantly over rest intervals. Furthermore, decoding ordinal positions of the sequence members (I.e., 5 class classification of 4-1-3-2-4) resulted in significantly higher accuracy (post: 94% and pre: 90% movement onset) compared to decoding the four finger identities.

Conclusion: This approach provides the most accurate strategy to date to decode individual actions from neural activity in the context of skill learning as required for identification of neural replay and optimization of control of BMI devices.

**Fig. 1:** Experimental Design

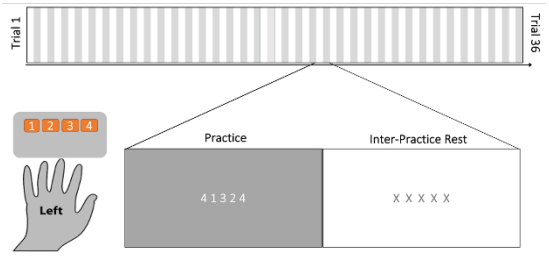


Fig 2: Contribution of ROIs in Decoding

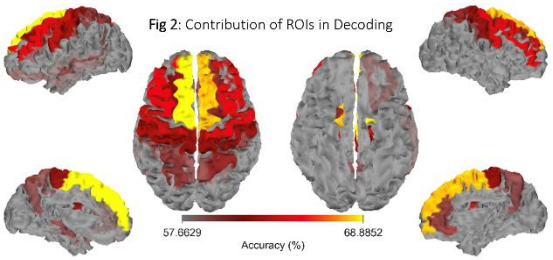


**Between-Trial representation difference and micro-offline gains**

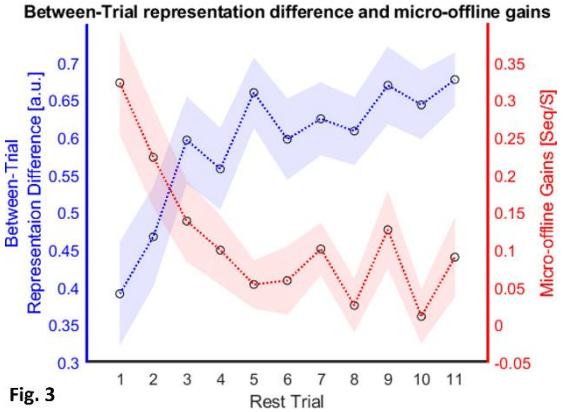


**Fig. 3**

**Fig.4: Confusion Matrix: Execution**

Accuracy = 94.15%; Weighted Mean F1 Score = 0.94
F1(Little) = 0.95; F1(Ring) = 0.94; F1(Middle) = 0.94; F1($Index_{OP1}$) = 0.94; F1($Index_{OPS}$) = 0.94

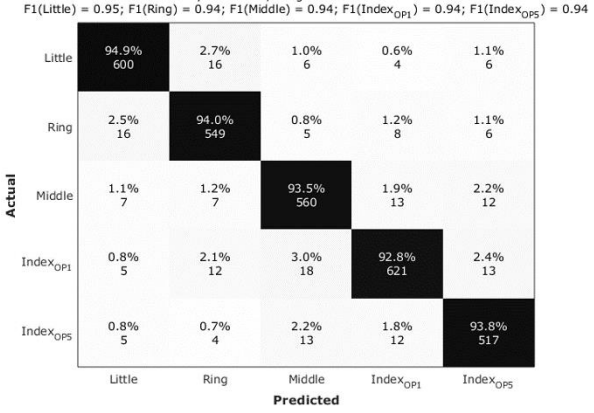

# Temporal Dynamics of Age, Gender, and Identity Representations Invariant to Head Views for Familiar Faces

Amita Giri [1,*], Grace Smith [1,*], Patrick Maloyan [1], Katharina Dobs [1,2], Amir Adler [1,3] and Dimitrios Pantazis [1]

[1]McGovern Institute for Brain Research, Massachusetts Institute of Technology, Cambridge, MA, USA

[2] Department of Psychology, Justus Liebig University Giessen, Giessen, Germany

[3]Electrical Engineering Department, Braude College of Engineering, Karmiel, Israel

[*]Authors contributed equally to this work

**Abstract**

Face recognition plays a crucial role in human social interactions by allowing us to identify and connect with others. In real-life situations, faces are encountered at various angles due to head movements. However, the neural mechanisms underlying the brain's ability to consistently recognize familiar faces across varied head view orientations remain poorly understood. Here, we employed MEG to explore the neural dynamics of face processing. Specifically, we used temporal decoding to differentiate age, gender, and identity, assessing how these attributes vary or remain invariant to head orientations for familiar faces.

We recorded MEG data while nineteen human subjects viewed face images of familiar identities and monitored for consecutive repetitions of identities (identity-based 1-back task) and identical images (image-based 1-back task). We chose twelve highly familiar US celebrities as identities, which varied orthogonally in gender and age, resulting in an equal distribution of six females and six males, as well as an even split between younger and older individuals. A total of 15 images per celebrity were selected, consisting of three distinct images for each of the five specified head views (direct, half left, full left profile, half right, and full right profile).

Decoding results for age, gender, and identity variant to head views are presented for both the identity-based and image-based tasks in Figures 1a and 1b, respectively. It is important to highlight that the identity-based task demanded a higher level of attention compared to the image-based task. This is consistent with the identity-based task exhibiting a sustained Area Under the Curve (AUC) over a longer duration compared to image-based task. Further, we found distinct timings for the emergence of different types of information. Specifically, both age (with peak times at 104ms in the identity-based task and 100ms in the image-based task) and identity information (with peak times at 108ms in both tasks) were decodable earlier than gender information. Gender information, on the other hand, exhibited a later emergence with peak times at 300ms in the identity-based task and 128ms in the image-based task.

To decode identity invariant to head view, a binary SVM classifier was trained with 5-fold cross-validation, each time using 4 head views for training and a left out view for testing. The fold-average time course for identity invariant to head view reached a peak at 112ms for both identity-based and image-based 1-back tasks (Figure 1c). Overall, our findings reveal the temporal dynamics of familiar face processing in humans, and offer valuable constraints for advancing computational models of face recognition.

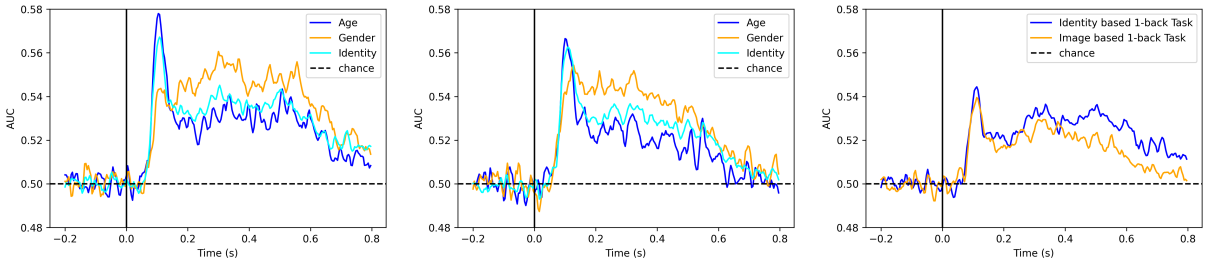


(a) (b) (c)

Figure 1: Temporal dynamics of age, gender, and identity *variant* to head view for (a) identity-based 1-back task and (b) image-based 1-back task. (c) Identity *invariant* to head view for both tasks.

Sebastian Montesinos

Laboratory of Brain and Cognition

**Temporal Characteristics of Mental Imagery**

Mental Imagery is the ability to perceive an image within one's mind in the absence of an external stimulus. The extent to which the mechanisms underlying perceptual processes overlap with those underlying mental imagery remains an open question. While some theories imply that mental imagery is generated from top-down mechanisms that impose representations across the visual system, others suggest that mental imagery involves the same bottom-up processes as in perception. To probe these theories, the present study used magnetoencephalography (MEG) to compare the time course of signals during perception and imagery. Participants viewed faces at different head orientations (looking left, centered, and looking right) and then imagined those same faces at the same set of orientations. Time-resolved MEG decoding methods allow us to compare brain MEG signal patterns between the different face orientations. In particular, we are comparing the ability to decode head orientation during both perception and imagery, as well as comparing cross-decoding between imagery and perception. Results from this study will help elucidate the evolving temporal characteristics of mental imagery.

**Load-dependent and capacity-limited response in the posterior parietal cortex during visual working memory retention: MEG evidence**

Xinchi Yu[1,2], Ellen Lau[1,2]

1- Neuroscience and Cognitive Science Program, University of Maryland, College Park

2- Department of Linguistics, University of Maryland, College Park

It has been established behaviorally that humans can only hold ~ 3 items in visual working memory (VWM; Luck & Vogel, 1997; Vogel & Machizawa, 2004). However, the biological basis of the VWM capacity is elusive. Prior fMRI studies have suggested that the posterior parietal cortex hosts load-dependent (increase as memory load increases) and capacity-limited (plateaus beyond the ~ 3 capacity) representations during VWM retention (Todd & Marois, 2004; Xu & Chun, 2006; Mitchell & Cusack, 2008; Robitaille et al., 2010). However, the slow modulation in blood signals makes it hard to disentangle perceptual encoding and VWM retention processes in fMRI. Only one existing MEG study examined this question (Robitaille et al., 2010), but a different paradigm from the fMRI studies was used. While the fMRI studies employed a central presentation paradigm (where the memorandum was presented around the center of the screen), the MEG study employed a bilateral presentation paradigm (where the memorandum was presented bilaterally and only one side was to be memorized based on a cue beforehand). In order to close the gap in the literature, we aim at testing if there are load-dependent, capacity-limited responses in the posterior parietal cortex with the central presentation paradigm, using MEG (Figure 1).

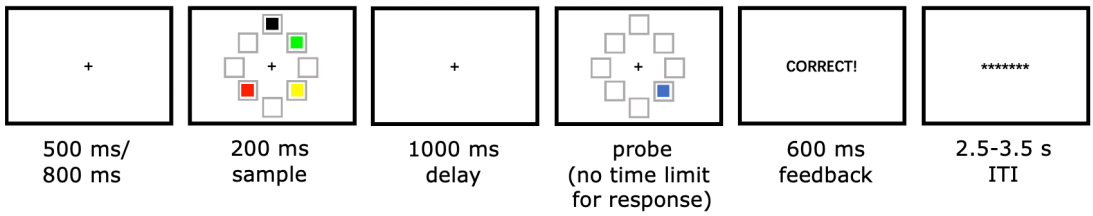


**Figure 1.** Illustration of a trial in our current experiment.

20 subjects entered data analysis. We performed source-space analysis using the dSPM method, and examined the mean response during encoding (0-400 ms) and VWM retention (400-1200 ms) periods in the posterior parietal cortex, the occipital cortex, and the anterior cingulate cortex (as a “sanity check”, cf. Todd & Marois, 2004). Indeed, the posterior parietal cortex hosted a load-dependent, capacity-limited response during VWM retention, but such effect was absent for encoding. In contrast, the occipital cortex demonstrated a load-dependent, capacity-limited response for encoding, but not during VWM retention. The anterior cingulate cortex did not show significant effects in either time windows. In all, we confirmed that the posterior parietal cortex is hosting load-dependent, capacity-limited responses during VWM retention. The observations in the occipital cortex also suggested that the visual cortex may not be compulsory for VWM retention, despite its importance in perceptual encoding.

# Exploring Working Memory Networks using Hidden Markov Models

Shivam Bansal, Jeff Stout, Fred Carver, Anna Namyst, Tom Holroyd, Amaia Benitez Andonegui, Allison Nugent

The human brain is a complex system that exhibits dynamic patterns of activity in response to external stimuli. Magnetoencephalography (MEG) is a noninvasive neuroimaging technique that has high spatial and temporal resolution to provide insight into these brain dynamics. However traditional MEG data analysis methods may not be able to identify rapid changes in functional networks. The classification of dynamic networks in a brain performing a task requires more complex modeling tools. In this study, we examine the use of hidden markov models (HMMs) to identify the presence of these networks in a working memory task. HMMs are probabilistic models that can capture the temporal dependencies and transitions between latent states that represent different network configurations. We hypothesized that HMMs would reveal distinct encoding and recall networks that involve the frontoparietal network, which is known to play a key role in working memory and executive function. Forty-two participants from the NIMH Healthy Volunteer dataset, a collection of neuroimaging and phenotypic data will be used in the study. The Sternberg working memory paradigm, which has an encoding phase where participants memorize a 4 or 6 letter string and a recall phase where participants must determine if a given probe was present in the string, was used to elicit encoding and recall networks. MEG data was collected via a 275 channel CTF scanner. MNE python was used to project data to the brain with LCMV beamformers and parcellation time series were constructed using the Desikan-Killiany atlas. The OSL Dynamics toolbox was used to orthogonalize the time series and compute the HMMs. The model was trained on the continuous data which was then epoched separately around when the string and the probe were shown. The average state activation vs time for an average epoch was generated along with the state power mapped on the brain for each state. The encoding-epoched and recall-epoched modes both displayed visual components approximately 100 ms post-stimulus. Separate left-dominant frontal and parietal components were also isolated in the encoding and recall models. The frontoparietal network was more active during encoding than recall, especially for higher memory load conditions. This study demonstrates the utility of HMMs to identify encoding and recall networks in working memory datasets. Results from this study can be used to inform future analysis of task-based data to classify dynamic brain networks.

# Estimating the Number of Active Sources in MEG Based on an F-ratio Method

Amita Giri [1,*], John C. Mosher [2], Amir Adler [3,1] and Dimitrios Pantazis [1]

[1]McGovern Institute for Brain Research, Massachusetts Institute of Technology, Cambridge, MA, USA

[2]Department of Neurology, Texas Institute for Restorative Neurotechnologies, UTHealth, Houston, TX, USA

[3]Electrical Engineering Department, Braude College of Engineering, Karmiel, Israel

**Abstract**

Magnetoencephalography (MEG) is a valuable method for investigating human brain function. Nevertheless, accurately determining the number of sources contributing to MEG recordings remains a difficult task due to factors like low signal-to-noise ratio (SNR), the existence of correlated sources, inaccuracies in modeling the head, and differences in individual anatomy. In response to these challenges, our research introduces a robust approach to precisely estimate the number of active sources within the brain. Our approach leverages the F-ratio statistical technique, enabling a direct comparison between a full model with $K+1$ number of sources and a reduced model with $K$ number of sources, where $K \in \mathbb{Z}$. We have developed a formal statistical procedure that incrementally increases the number of sources in the context of the multiple dipole localization problem until all relevant sources are identified. The flowchart of the F-ratio method is shown in Figure 1. Our findings reveal the importance of selecting appropriate thresholds, which must be adjusted in accordance with the number of sources and SNR levels. Interestingly, these thresholds remain relatively stable for factors such as inter-source correlations, inaccuracies in translational modeling, and diverse cortical anatomies. By identifying the optimal thresholds and confirming the effectiveness of our F-ratio-based approach using simulated, actual phantom, and real human MEG data, we illustrated the superiority of our method over established statistical techniques like the Akaike Information Criterion (AIC) and Minimum Description Length (MDL). In summary, when fine-tuned for threshold selection, our method provides researchers with a reliable tool for estimating the genuine count of active brain sources and faithfully representing brain function.

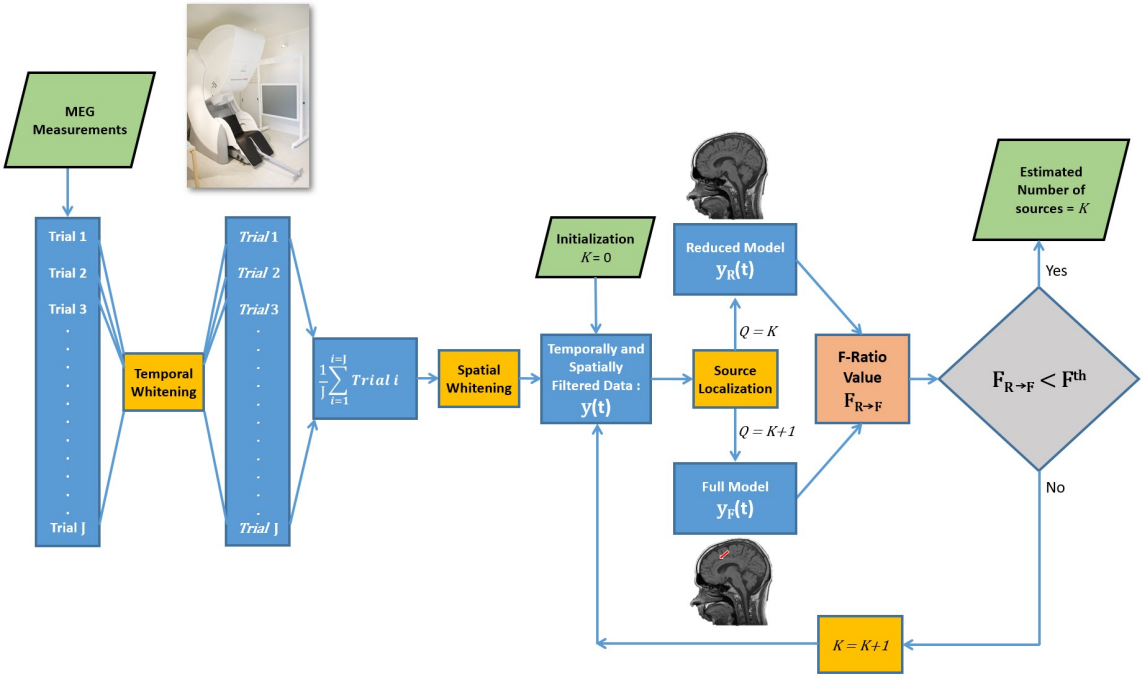


Figure 1: Flowchart of the F-ratio method for estimating the number of sources.

**Multi-Modal Deep Fusion Neural Networks for Brain Source Imaging Based on EEG and MEG**

**Meng Jiao, Shihao Yang, Feng Liu**
**Stevens Institute of Technology**
**Hoboken, NJ, 07030, USA**

Electrophysiological Source Imaging (ESI) aims to reconstruct the underlying electric brain sources based on Electroencephalography (EEG) or Magnetoencephalography (MEG) measurements of brain activities. Due to the ill-posed nature of the ESI problem, faithfully recovering the latent brain sources has been a significant challenge. Classical algorithms have primarily focused on the design of regularization terms according to predefined priors derived from neurophysiological assumptions. Deep learning frameworks attempt to learn the mapping between brain source signals and scalp EEG/MEG measurements in a data-driven manner, and have demonstrated improved performance compared to the classical methods. Given that EEG and MEG can be complementary for measuring the tangential and radial electrical signals of the cortex, combining both modalities is believed to be advantageous in improving the reconstruction performance of ESI. However, the fusion of these two modalities for the ESI problem has not been fully explored in existing deep learning frameworks. In this paper, we propose a Multi-Modal Deep Fusion (MMDF) framework for solving the ESI inverse problem, termed as MMDF-ESI. Our framework integrates both EEG and MEG in a deep learning framework with a specially designed squeeze-and-excitation module. This integration of EEG and MEG is conducted at an early phase in the deep learning framework rather than on the final decision level fusion. Our experimental results show that (1) the localization accuracy of MMDF-ESI consistently outperforms that of using a single modality; (2) MMDF-ESI exhibits excellent stability, characterized by significantly smaller error variance in source reconstruction compared to benchmark methods, particularly for sources with larger extended activation areas and under low signal-to-noise ratio (SNR) conditions; (3) the evaluation on a real EEG/MEG dataset demonstrates that MMDF-ESI enables a more concentrated reconstruction, effectively recovering an extended area of underlying source activation.

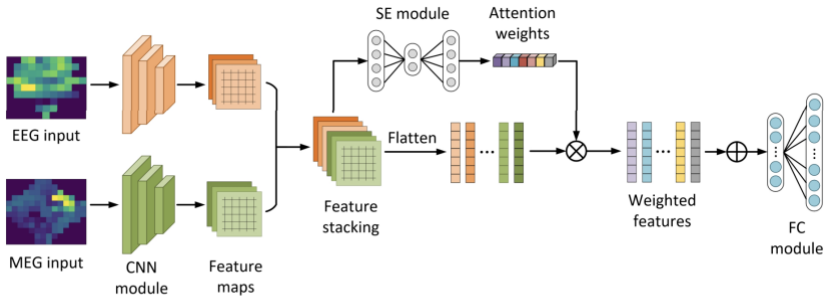


Fig. 1: The proposed framework architecture.

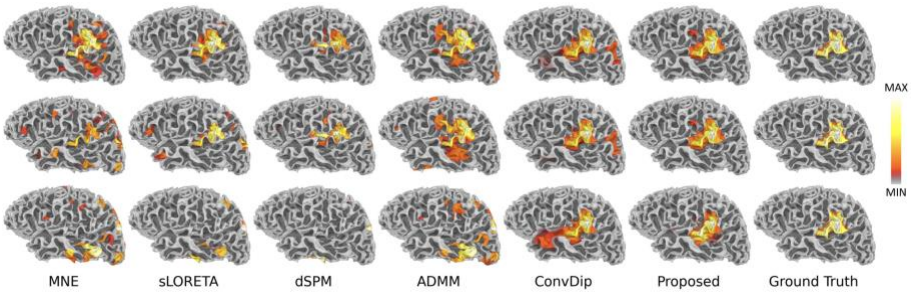


Fig. 2: the comparison of different performance result

**Bayesian Inference for Brain Source Imaging with Structured Low-rank Noise**

**Authors:**
Sanjay Ghosh[a] , Chang Cai[b] , Ali Hashemi[c], Yijing Gao[a], Stefan Haufe[c], Kensuke Sekihara[d], Ashish Raj[a], Srikantan S. Nagarajan[a]

[a]University of California San Francisco, San Francisco, USA.
[b]Central China Normal University, Wuhan, China.
[c]Technical University Berlin, Berlin, Germany.
[d]Signal Analysis Inc., Tokyo, Japan.

**Presenter:** Dr. Sanjay Ghosh, Postdoctoral Scholar, University of California San Francisco.
(**Dr. Ghosh would like to be considered for a travel award.**)

**Abstract**: *Objective*: The inverse problem in brain source imaging is the reconstruction of brain activity from non-invasive recordings of electroencephalography (EEG) and magnetoencephalography (MEG). One key challenge is the efficient recovery of sparse brain activity when the data is corrupted by structured noise that is low-rank noise. This is often the case when there are a few active sources of environmental noise and the MEG/EEG sensor noise is highly correlated. *Approach:* In this work, we propose a novel robust empirical Bayesian framework which provides us a tractable algorithm for jointly estimating a low-rank noise covariance and brain source activity. Specifically, we use a factor analysis model for the structured noise, and infer a sparse set of variance parameters for source activity, while performing Variational Bayesian inference for the noise. *Main results and significance*: We perform exhaustive experiments on both simulated and real datasets. Our algorithm achieves superior performance as compared to several existing benchmark algorithms for brain source imaging. One key aspect of this algorithm is that it does not require any additional baseline measurements to estimate the noise covariance from the sensor data.

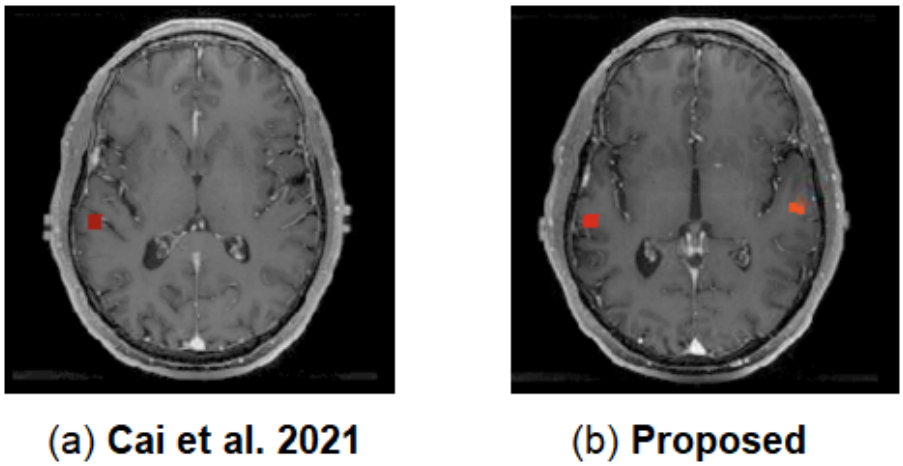


*Figure 1*: Brain source imaging on real MEG data for auditory evoked field (AEF) stimulation. Notice that the proposed method could localize bilateral auditory activity more efficiently.

**Reliable MEG/MSI source localization in patients with implanted vagus nerve stimulator (VNS) devices: a single-centered, large clinical observation study**

Mahmoud Jiha[1], Velmurugan Jayabal[1], Dylan Davis[1], Gavin Belok[1], Joshua Chon[1], Srivatsan Tennathur[1], Chang Cai, Mary Mantle[1], Anne Findlay[1], Heidi E. Kirsch[1], and Srikantan S. Nagarajan[1]

**Background**: A subset of medically refractory epilepsy patients undergo VNS implantation to minimize their seizure burden. Some of these patients do not respond to VNS stimulation or have persistent seizures; hence they are subsequently evaluated with MEG to identify the potential epileptogenic zone (EZ) for possible surgery. However, VNS devices induces persistent artifact in the raw MEG data; large-amplitude fluctuations which hinder and mask the ongoing background brain activity. Here we present our clinical experience on the utility of the dual-signal subspace projection (DSSP) algorithm in decontaminating such artifacts and identifying and localizing the interictal epileptiform discharges (IED).

**Method**: We included 117 patients (66 males, 51 females) with implanted VNS who underwent simultaneous MEG/EEG between November 2004 and July 2023 at the University of California, San Francisco Biomagnetic Imaging Laboratory. Patient ages ranged from 4.3 to 69.3 years (M = 32.4, SD = 14.5). Of these 117 patients with VNS, only 66 patient's (56.4%) MEG data was pre-processed with DSSP to remove VNS induced artifacts. To compare the effectiveness of our approach, we randomly included another cohort of 117 epilepsy patients (72 males, 45 females) without VNS implant who had undergone MEG/EEG between November 2004 and July 2023. In this cohort, patient ages ranged from 1.5 to 74.6 years (M = 24.6, SD = 14.7). The raw MEG data was visually reviewed for both cohorts and the following information were qualitatively interpreted as follows; 1) Presence or absence of any IED detection in the pre and post DSSP (if any) processed MEG data; 2) Successful or unsuccessful equivalent current dipole (ECD) source modeling of at least one IED. Between group (with and without VNS) and within VNS group (with and without DSSP) statistical analyses were performed using chi-squared test at the 0.05 significance level.

**Results**: In patients with implanted VNS, utilization of DSSP to decontaminate the raw data did not increase the likelihood of IED detection (p=0.47) when compared with patients where DSSP was not used. However, DSSP significantly improved ECD source localization of detected IEDs (76% vs 56%; $X^2$ = 4.68; p=0.03), in comparison to source localization of events on the non-DSSP data. It is interesting to note that both the ability to detect IED (p=0.73) and ECD source localization (p=0.39) in VNS patients was comparable with the general MEG population without VNS.

**Significance**: The current study attempts to provide deep insight into the clinical utility of MEG/MSI source localization in the large cohort of VNS patients amidst persistent artifacts. We demonstrated that DSSP artifact rejection improved the detection and localization accuracy of these epileptifom events.

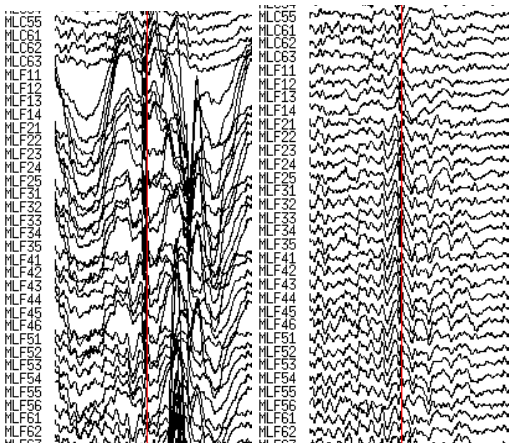

*Figure-1: The figure demonstrates the raw MEG data with large amplitude VNS artifacts (left) and after being processed with DSSP, showing events without any artifacts (right)*

**Validation of a novel hand-squeezing paradigm for quantification of interhemispheric inhibition (IHI) between motor cortices using MEG**

Alica Rogojin, Alisha Ahmed, Jed Meltzer

**Background:** Several neuroimaging studies of motor control have demonstrated differences in brain activation patterns between stroke patients and healthy controls. Normally, during unilateral motor performance the contralateral primary motor cortex (M1) inhibits the ipsilateral hemisphere. When the contralateral M1 is affected following stroke, inhibition of the ipsilateral hemisphere is lost and results in the increased activation of the contralesional (unaffected) M1. This elevated neural activation in the contralesional hemisphere may be evidence of that hemisphere taking over function in a helpful manner, but may also represent a pathological, maladaptive process that should be suppressed. Currently, there is much interest in the increased interhemispheric inhibition (IHI) of the injured hemisphere following stroke, and how it pertains to functional recovery. This highlights the importance of a physiological measure that will allow us to quantify IHI between motor cortices. MEG studies have shown that slow oscillatory activity can be localized specifically to perilesional tissue, as well as a general "slowing" of electrical activity in stroke patients. Based on these findings, MEG-derived measures of spectral slowing could be used as an outcome measure in stroke intervention studies. **Objectives:** The goal of the current study is two-fold: 1) to validate a novel hand-squeezing paradigm, and 2) to use it to characterize an oscillatory marker in MEG that will allow us to quantify IHI between motor cortices and possibly beyond. Given that we eventually want to use this paradigm in stroke patients who may lack the dexterity to push a button with a single finger, we instead use a whole hand squeezing motion performed with a grip force transducing lever. **Methods:** The study paradigm includes right unilateral, left unilateral, in-phase (simultaneous) bilateral, and anti-phase (alternating) bilateral hand squeezes performed at 3 different frequencies (0.5, 1, 2 Hz). In previous fMRI research, similar protocols with continuous finger tapping movements were found to create an ipsilateral deactivation that increases with tapping frequency during dominant right-hand movement. Moreover, research has found reduced non-dominant to dominant motor cortex IHI during in-phase bilateral movement. In anti-phase movements, IHI from moving to non-moving M1 is needed to prevent mirror movement. By including in-phase and anti-phase bilateral movements in our experiment, we will be able to characterize IHI using MEG. A pilot dataset from one right-handed healthy young adult subject was collected for protocol validation. Synthetic aperture magnetometry (SAM) was performed to investigate power differences in the beta-band frequency (15-30 Hz) between conditions (T-value > 2.5). **Results:** Preliminary SAM results show stronger ERD in the right M1 during left-hand movements compared to right-hand movements at slow and fast movement frequencies. Instead of ERD in the left M1 for right- compared to left-hand movements, as might be expected, there was more beta ERD in the left M1 when moving the left hand. This may indicate that the left M1 is involved in moving both hands, and may reflect the brain requiring more neural resources to move the non-dominant hand. Slow frequency anti-phase vs in-phase movements show bilateral M1 ERD. This may indicate that the task is more demanding (more suppressive of beta) in the anti-phase condition, even though there is less raw movement (with both hands moving at 0.5 Hz, each hand in the anti-phase condition is actually moving at 0.25 Hz). **Discussion:** The pilot results validate the use of a continuous hand-squeezing paradigm for evaluating MEG activity in the motor cortex in healthy adults, and may be extended for future research involving stroke patients with upper limb impairments.

# Multi-Frequency Encoded Source Imaging for Wearable OPM-MEG

*J Xiang, N Hemasilpin, J Jiang, J Bonnette, M Anand, C Riehm, B Schlink, J Diekfuss, G Myer*

*MEG Center, Cincinnati Children's Hospital Medical Center, University of Cincinnati,*
*3333 Burnet Avenue, Cincinnati, OH*
*Email: Jing.xiang@cchmc.org*

Despite the existence of high-frequency brain signals (HFBS, ≥70 Hz) up to 8,000 Hz, it is worth noting that low-frequency brain signals (LFBS, <70 Hz) are the primary focus in clinical applications. One issue is the relative weakness of HFBS, which frequently necessitates their acquisition via intracranial recordings. Furthermore, localizing HFBS is a daunting task. Our goal was to create a novel magnetoencephalography (MEG) system that used optically pumped magnetometers (OPMs) for noninvasive detection and localization of both LFBS and HFBS.

A novel prototype of a wearable OPM MEG was constructed utilizing a helmet composed of two layers. A series of techniques, such as synthetic gradiometers (SGs), frequency-specific signal space classification (FSSSC), and artificial intelligence (AI) techniques, were devised to mitigate the effects of motion artifacts and environmental noise. Four software packages have been developed to facilitate various aspects of MEG data process, including data acquisition, paradigm design, data analysis, and source localization. To examine brain activities across a wide range of frequency bands, we have devised frequency-encoded source imaging (FESI). Both OPM MEG and superconducting quantum interference device (SQUID) MEG data were obtained from phantoms and human subjects.

MEG data showed that OPMs consistently detected HFBS. In wearable OPM MEG, SGs and FSSC significantly reduced artifacts and noise. The strength of OPM neuromagnetic signals is 3.6-9.1 times that of SQUID neuromagnetic signals. FESI successfully localized brain signals in a variety of frequency bands ranging from low to high frequencies (Fig. 1). A new OPM MEG method based on AI could analyze OPM MEG data automatically.

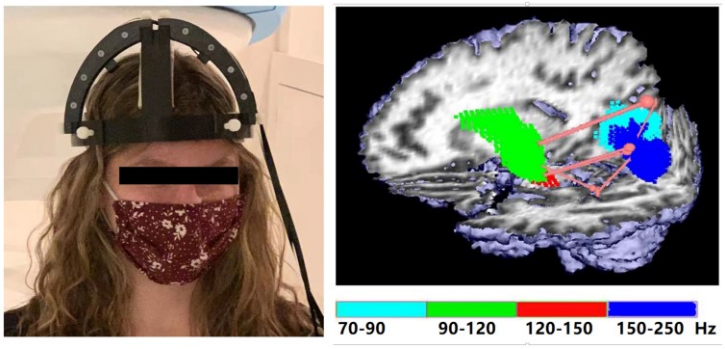


**Fig. 1. A Photo of a Wearable OPM MEG Prototype and Frequency-Encoded Source Imaging from a Participant.** High-frequency brain signals (HFBS, ≥70 Hz) are detectable by OPM and SQUID MEG. When extracting HFBS, a new software solution can get rid of noise and artifacts. Brain activity is only visible in one frequency band in conventional source imaging. The new FESI displays brain activity across multiple frequency bands. According to the pilot data, HFBS are localized to language areas.

The findings show that OPM MEG is wearable, non-cryogenic, low-cost, and outperforms SQUID MEG. OPM MEG can detect HFBS, and a software solution can reduce artifacts and noise significantly. FESI can detect and visualize brain activity from low to high frequency bands, as well as provide novel cross-frequency information (Fig. 1). A combination of wearable OPM-MEG and HFBS has the potential to alter the landscape of brain research. Wearable OPM MEG detection of HFBS may pave the way for future brain disorder diagnosis and treatment.

# Biplanar coil cancellation system for OPM-MEG using PCB

Mainak Jas, Yoshio Okada, John Kamataris, Teppei Matsubara, Chunling Dong, Padmavathi Sundaram

Optically pumped magnetometers (OPMs) are a promising sensor technology for non-invasive on-scalp measurement of human electrophysiological signals. OPM-MEG offers the potential for higher spatial resolution, naturalistic MEG studies involving movements, and higher signal-to-noise ratio (SNR) for superficial cortical sources. Despite these potential advantages, OPMs are yet to be widely adapted, in part due to the difficulty of operating the sensors in lightly shielded environments. OPM sensors need to operate in a zero background field to achieve linearity and minimize signal distortion. Several groups have proposed active field cancellation coils [1] to remove the constant and gradient components of the magnetic field. As opposed to traditional Helmholtz (or anti-Helmholtz) coil designs, these biplanar coils allow subjects to follow instructions, perform visual tasks with an unobstructed front view, as well as perform movements within a predefined region.

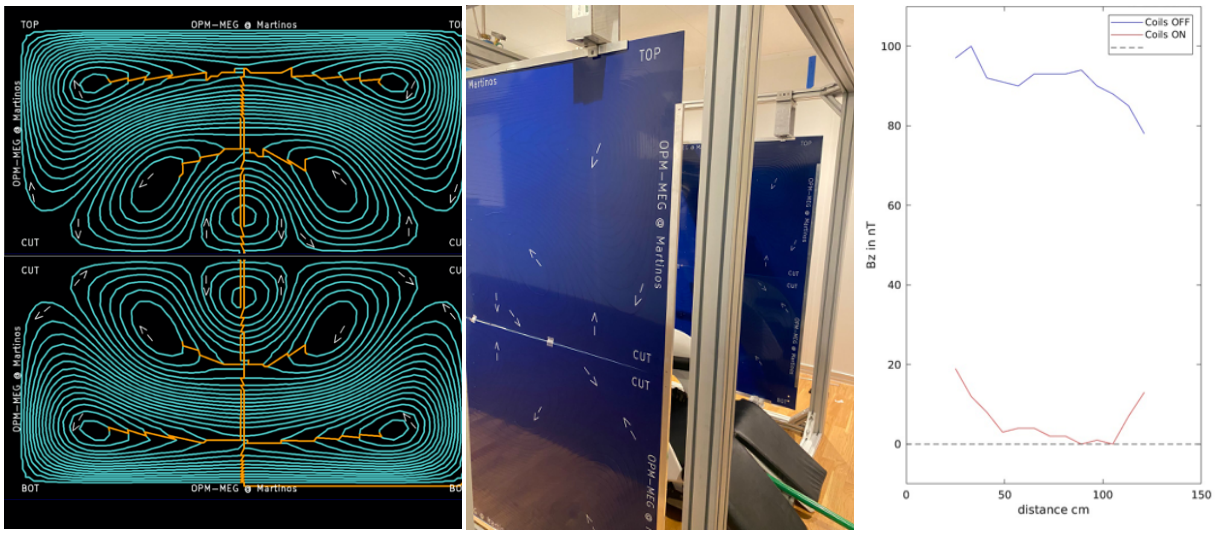


**Fig 1. A.** Optimized coil design for printed circuit board (PCB), and **B.** Installed PCB inside a one-layer shielded room at the Martinos Center, MGH, and **C.** Background field profile between the coil centers before and after the coils are turned on. Remnant ~6 nT/m gradient field was not canceled by this coil.

However, until now, biplanar coils were error-prone and expensive to manufacture, involving manual winding of >1000 meters of copper wire. In this work, we created a field cancellation coil on a two-layer Printed Circuit Board (PCB) for one component (floor to ceiling) of the magnetic field in a one-layer shielded room. We used the open source bfieldtools [2] package to optimize and discretize the current loops that produce a constant magnetic field in a target region. The discretized coils were connected into a continuous path (**Fig 1A, cyan: Layer1; orange: Layer 2**) using an in-house interactive interface. The coil pairs were manufactured on two 1.5 m x 0.75 m PCBs (2 oz copper) and soldered together. The PCB coils were mounted on a sliding aluminum frame for easy access to the subject during experiments (**Fig 1B**). The theoretical efficiency of the coils was 1.15 nT/mA and we obtained an efficiency of ~1 nT/mA experimentally. We measured 7 ohms resistance per coil, compared to the theoretical 5.2 ohms. Preliminary results suggest that PCB cancellation coils are more accurate than hand-wound coils and can be easily replicated and mass-manufactured at a lower cost. This innovation paves the way for cheaper and more robust commercial OPM-MEG systems.

## References

1. Holmes, N., Leggett, J., Boto, E., Roberts, G., Hill, R. M., Tierney, T. M., ... & Bowtell, R. (2018). A bi-planar coil system for nulling background magnetic fields in scalp mounted magnetoencephalography. *Neuroimage*, *181*, 760-774.
2. Zetter, R., J Mäkinen, A., Iivanainen, J., Zevenhoven, K. C., Ilmoniemi, R. J., & Parkkonen, L. (2020). Magnetic field modeling with surface currents. Part II. Implementation and usage of bfieldtools. *Journal of Applied Physics*, *128*(6).

**Acknowledgements:** This work was supported by NIH grants P41EB030006, 5R01NS104585, 1R01NS112183, and 2R01NS104585-05.

**Title**: OPM-MEG vs. SQUID-MEG in Epileptic Source Localization: A Cost-Effective Alternative

**Authors**: Tyrell Pruitt PhD, Natascha Fonseca PhD, Sasha Alick-Lindstrom MD, Pegah Askari, Amy L. Proskovec PhD, Joseph A. Maldjian MD, and Elizabeth M. Davenport PhD

**Affiliations**: The University of Texas Southwestern Medical Center, Department of Radiology, Dallas, Texas, USA

**Rationale**: Superconducting quantum interference device magnetoencephalography (SQUID-MEG), renowned for its precision, is financially and operationally burdensome due to its liquid helium requirements. This study scrutinizes optically pumped magnetometer magnetoencephalography (OPM-MEG), characterized by a low sensor count (10) and helium-free operation, as a cost-effective and efficient alternative.

**Methods**: Patients (n = 8) were subjected to sequential SQUID-MEG and OPM-MEG scans. For the SQUID-MEG scans, a traditional clinical protocol was followed. Subsequently, a supplementary protocol was administered using the OPM-MEG system. This supplementary protocol involved a series of tasks designed to stimulate different regions of the brain: a 5-minute resting period, a 2-minute epoch baseline, a motor task, a visual task, and a language task. Localization results from both systems were juxtaposed for direct comparison. Epileptic spikes were identified by a neurophysiologist and modeled using traditional dipole modeling in clinical software for SQUID-MEG, and Linearly Constrained Minimum Variance (LCMV) beamforming in Brainstorm software for OPM-MEG.

**Results**: OPM-MEG localized tasks and spikes effectively, yielding comparable but not equivalent results to SQUID-MEG. Visual representations substantiate the relative efficacy of both systems. Furthermore, SNR calculations revealed that low sensor count OPM-MEG and traditional SQUID-MEG have comparable SNR in a shielded environment. (14.5 db to 15.1 db respectively)

**Conclusions**: OPM-MEG serves as a financially viable alternative to SQUID-MEG, particularly in settings with resource constraints. Its comparable performance in both localization and SNR could democratize access to essential neuroimaging tools, thereby expanding the scope of epilepsy research and treatment.

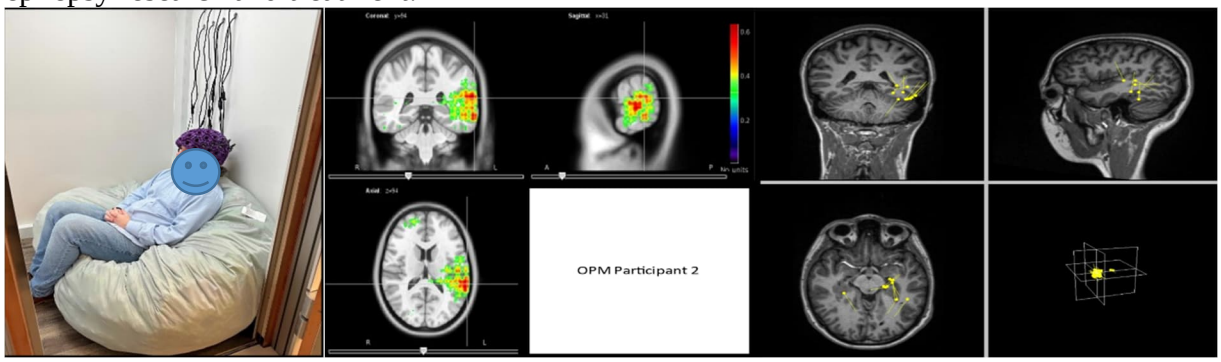


[Figure 1: OPM-MEG rigid helmet system (Left) and participant sitting comfortably in the MSR with the helmet on prior to an experiment. Comparison of spike localization results from OPM-MEG (Middle) and SQUID-MEG (Right) localizations in patient 2. LCMV beamformer was used in the Brainstorm software package for the OPM-MEG localization and the traditional dipole modeling was used for the right SQUID-MEG image.]

# Towards precise mapping of digit representations in the human somatosensory cortex with high resolution magnetoencephalography

Amaia Benitez-Andonegui, Riley Hochstein, Anna Namyst, Frederick Carver,
Shivam Bansal, Tom Holroyd, Stephen Robinson, Allison Nugent
*Magnetoencephalography Core, NIH, Bethesda*

**Introduction.** Optically pumped magnetometers (OPMs) have emerged as an alternative to SQUID-based MEG, as they can be more robust to motion artifacts, and can be brought very close to the scalp, thus offering increased sensitivity (Knappe et al., 2016). Previous work developing OPM arrays focused on whole-head arrays to replace traditional MEG systems (Boto et al., 2020; Hill et al., 2020). The current work focuses an OPM array that is spatially dense and optimized to resolve cortical activity in a small patch of cortex. Since the spatial and temporal resolution of our method approaches that of ECoG, we refer to as *magnetocorticography (MCoG)*. Simulation studies from our group suggest that spatially dense OPM arrays can outperform traditional whole-head SQUID-based MEG systems in the detection and localization accuracy of nearby neural sources (Nugent et al, 2022). In the present study, we aimed to assess the capabilities of our OPM array empirically. **Methods.** We measured somatosensory evoked fields (SEF) using pseudo-randomized application of air pulses to the right index, middle and ring fingertips. Six participants received 160 pulses to each finger over 4 runs, with a variable inter stimulus interval (mean= 2.5s, jitter ±500ms). The OPM array was placed and fixated over the left somatosensory cortex, and coregistered to subject-specific MRIs using BrainSight. Four of our six participants underwent a whole-head SQUID-MEG session with the same stimulation paradigm for comparison purposes. All MEG data were filtered to remove the effect of power mains and bandpass filtered (1Hz-95Hz) before epoching data (from -0.3 to1.7 s after stimulus onset). **Results.** SEFs recorded with OPM sensors were larger than SQUID sensors (mean peak 550fT vs 200fT across subject and digits). In addition, we carried out dipole fitting of the early component of the SEFs (30-60ms after stimulus onset). Bootstrapped resampling was used to quantify the accuracy of the estimated dipole sources (with n=1500 iterations). Median goodness-of-fit values ranged between 62.8% and 95.9% for OPM-MEG (72.1%-95.1% for SQUID-MEG), while median dipole amplitudes ranged between 19.2 and 56.2 nA-m for OPM-MEG (20.1-56.3 nA-m for SQUID-MEG) across participants and digits. Mean localization accuracy of dipole sources resulted in similar confidence radii (Jamali and Ross, 2012) across MEG modalities in the left somatosensory cortex (7.1 mm for OPM-MEG vs 5.9 mm for SQUID-MEG, measured across subject and digits) and mean percent overlap between digits (67% overlap for OPM-MEG vs 45% overlap for SQUID-MEG); see Figure 1 for estimated dipole locations and overlap across digits and MEG modalities in one participant. **Conclusion.** Our results show promising localization capabilities of our OPM-MEG array. Future analyses will assess the effect of artifact reduction techniques such as ICA on dipole fitting routines for OPM sensors, together with assessing the agreement between LCMV beamformed images and dipole fits.

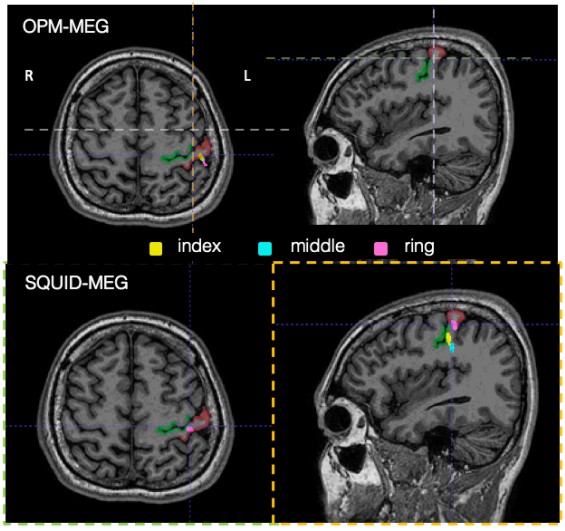


*Figure 1. Example of bootstrapped dipole fit locations for each digit and both MEG modalities (single participant).*